THE UNIVERSITY OF MICHIGAN
MAY 31 1960
ENGINEERING LIBRARY

Journal of the Institute of Petroleum

VOL. 46 MARCH 1960 No. 435

CONTENTS

63 **The Hydrodynamic Effect between Approaching Surfaces with Interposed Viscous Fluid Films, and its Influence on Surface Deformations**
By L. H. Butler

74 **South African Shale-Oil Bitumen as a Road Binder**
By E. J. Dickinson

84 **Removal of Impurities which Lower the Electrical Breakdown Strength of Transformer Oil by Distillation**
By M. Darveniza

89 **Estimation of Relative Maximum Depths of Burial**
By G. D. Hobson

Abstracts 320–494

Book Reviews

Additions to the Library

PRICE 10s 0D A COPY OR £4-14-6 YEARLY *POST FREE*

Published by the Institute of Petroleum 61 New Cavendish Street London W1

Printed in Great Britain by Richard Clay and Company Ltd Bungay Suffolk

COUNCIL, 1959–60

President

C. M. Vignoles, C.B.E., M.A.

Immediate Past-President

The Rt. Hon. Lord Geddes, C.B.E., D.L., M.A.

Vice-Presidents

C. Chilvers, B.Sc., F.R.I.C. H. Hyams T. W. Mathias, O.B.E., M.A.

Members of Council

J. G. Annan, B.Sc.
V. Biske, B.Sc., LL.M., F.R.I.C.
G. A. Dickins, B.Sc.(Hons), F.R.I.C., M.Am.Chem.Soc.
E. J. Dunstan, M.Sc., M.I.Chem.E.
A. J. Foster
F. L. Garton, M.A., B.Sc.
Sir Stephen Gibson, C.B.E., M.A., M.I.Mech.E.
R. H. W. Hamilton, M.A.
L. L. Hosking, B.E., M.I.C.E., A.M.N.Z.I.E.
M. E. Hubbard, B.A., M.I.Mech.E.
C. S. Newey, B.Sc.
K. E. W. Ridler, Ph.D.
D. L. Samuel, B.Sc., A.R.I.C.

Representing the Branches Committee

C. W. Banyard, B.Sc.(Eng.) J. H. M. Clark, T.D., A.C.A.
D. H. Tullis, B.Sc., A.R.T.C., A.R.I.C., M.I.Chem.E.

Honorary Treasurer

O. F. Thompson, O.B.E.

Honorary Secretary

W. M. Catchpole, M.A.

Honorary Editor

E. B. Evans, M.Sc., Ph.D., F.R.I.C.

Honorary Associate Editor

D. L. Samuel, B.Sc., A.R.I.C.

General Secretary

D. A. Hough, T.D., F.I.A.C.

Editor

George Sell

Honorary Secretaries of Branches

Bahrain Branch: D. G. Johnstone, c/o Bahrain Petroleum Co. Ltd., Awali, Bahrain, Persian Gulf.
Essex Branch: D. Rawlinson, F.R.I.C., c/o Shell Refining Co. Ltd., Shell Haven, Essex.
Fawley Branch: C. W. Banyard, B.Sc.(Eng.), c/o Esso Petroleum Co. Ltd., Fawley, Southampton.
Kuwait Branch: G. A. Lee, c/o Kuwait Oil Co. Ltd., Ahmadi, Kuwait.
London Branch: J. H. M. Clark, T.D., A.C.A., c/o Mobil Oil Co. Ltd., Caxton House East, Westminster, S.W.1.
Northern Branch: H. Kaye, B.Sc., A.M.I.Chem.E., c/o Manchester Oil Refinery Ltd., Twining Road, Trafford Park, Manchester 17.
Scottish Branch: W. M. Stirling, A.H-W.C., A.M.I.E.E., Scottish Oils Ltd., Middleton Hall, Uphall, Broxburn, W. Lothian.
South-Eastern Branch: D. K. L. Morgan, B.Sc., c/o BP Refinery (Kent) Ltd., Isle of Grain, Rochester, Kent.
South Wales Branch: G. L. Jenkins, BP Refinery (Llandarcy) Ltd., Llandarcy, Glam.
Stanlow Branch: A. S. Brooman, B.Sc., 11 Grange Crescent, Hooton, Wirral, Cheshire.
Trinidad Branch: H. C. Hobson, c/o Apex (Trinidad) Oilfields Ltd., Fyzabad, Trinidad, B.W.I.
Yorkshire Branch: A. Furness, c/o J. W. Miller and Son Ltd., Hillside Oil Works, Brighouse, Yorks.

THE HYDRODYNAMIC EFFECT BETWEEN APPROACHING SURFACES WITH INTERPOSED VISCOUS FLUID FILMS, AND ITS INFLUENCE ON SURFACE DEFORMATIONS *

By L. H. BUTLER †

SUMMARY

The pressure distributions in the fluid film between rigid surfaces approaching at constant velocity are calculated. Various surface profiles are assumed and allowance is made for variation of fluid viscosity with pressure. The implications in the case of flat and parallel approaching faces are discussed at some length, since they demonstrate clearly the marked influence of the pressure–viscosity dependence. Whilst the problem is of interest in its own right, the discussion is extended to show that fluid films may be established in continuous metal deformation processes. It is suggested that the presence of such films may lead to the surface deterioration of the deformed metal sometimes observed experimentally. In the appendix a further extension is considered in which the deforming surface is receding with a velocity varying across its profile. The pressure distribution in such a case supports the previous hypothesis of the establishment of a full fluid film.

Symbols

x, y, z	Cartesian co-ordinate directions.
r, θ	Polar co-ordinates.
$2R$	Diameter of approaching disks.
h	Gap between disks at any instant at radius r (=constant = h_1 in the case of flat and parallel approaching faces).
$V = -\frac{dh}{dt}$	Velocity of approach of faces at any instant.
η	Fluid absolute viscosity (a function of pressure).
η_0	Fluid viscosity at atmospheric pressure—initial viscosity.
$p_1, p_2, \ldots$ etc.	Fluid pressure in the film.
$\bar{p}_1, \bar{p}_2, \ldots$ etc.	Mean fluid pressures.
$p_{1\max}, \ldots$ etc.	Maximum fluid pressures.
m	Pressure viscosity index.
k	A parameter $= \frac{12V\eta_0}{h_1^3}$.
$W_1, W_2, \ldots$ etc.	Total supported loads.
H	Instantaneous maximum gap.
h_p	Instantaneous peripheral gap.
α, β	Profile constants.
v	Instantaneous velocity of deforming surface at radius r (Appendix).
a, b	Velocity coefficients (Appendix).

Fig 4 shows the geometrical configuration.

INTRODUCTION

WHEN relative motion exists between two adjacent surfaces separated by a fluid film, and the geometrical configuration of the system is suitable, it is accepted that complete separation of the surfaces can be maintained on the basis of Reynolds' [1] hydrodynamic theory. In extreme cases, investigations, *e.g.* those of McEwen [2] and Cameron [3] on gear tooth lubrication, indicate that such films may be present under very severe loading conditions. Such work has stimulated interest in the elasto-hydrodynamic problem, in which allowance must be made for the elastic deformation of the surfaces under the influence of the fluid pressure generated. The solution of such problems presents some difficulty, since the equations determining the generation of the fluid pressure, and the elastic deformation of the surfaces, must be compatible. A recent contribution in this field is due to Dowson and Higginson,[4] in which a numerical solution is obtained for the case of a disk running inside a ring, allowance being made for fluid viscosity varying with pressure.

An extension to the general elasto-hydrodynamic problem may be readily visualized in which the surface deformation may extend beyond the elastic to the plastic range, conditions which may well occur under suitable operating conditions in metal deformation processes. Illustration and an analytical discussion of this effect for free falling, impacting lubricated surfaces is contained in the work of Bowden and Tabor,[5] assuming a fluid of constant viscosity. Whilst it is not proposed here to attempt the analytical solution for the general problem, it is intended to demonstrate that similar effects may occur under very moderate approach conditions, allowing additionally for the fact that viscosity may be pressure dependent.

The geometrical configuration taken is that appropriate to a simple compression test in which a cylindrical flat-ended specimen is compressed between flat dies. In a series of such experiments [6, 7] various lubricants were interposed between the die and specimens. Some unusual surface effects were observed on the specimen end faces which could most satisfactorily be explained on the basis that a continuous or semi-continuous lubricant film was maintained throughout the compression process.

It was shown that if the mating specimen and die faces are initially highly polished, the appearance of the specimen contact faces after deformation is markedly influenced by the viscosity of the interposed lubricant. If no lubricant or one of low viscosity is used, the specimen becomes virtually a replica of the die, and thus appears highly polished. With heavier

* MS received 21 December 1959.

† University College, Cardiff.

lubricants, however, the surface takes on a matt, non-reflective appearance over the greater part of the contact area with, usually, a burnished narrow annular ring appearing at the contact periphery (Figs 1–3). The non-reflective area shows a deformed surface texture apparently closely related to the original grain structure of the deformed metal, and it has been suggested that deformation occurs initially largely via a continuous fluid film trapped at the interface, allowing individual grains to deform in a preferred manner.

A simple analysis has been given [7] in which the pressure distribution in the film was calculated. It was shown that a pressure distribution (parabolic)

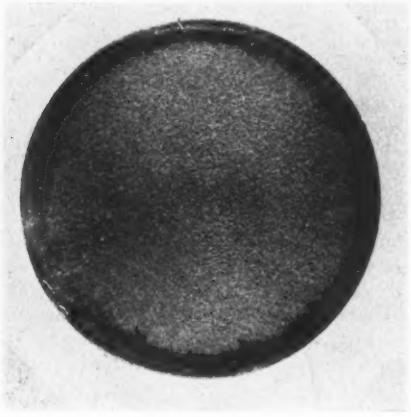

FIG 1

MILD STEEL × 2

The original material has a fine grain size.

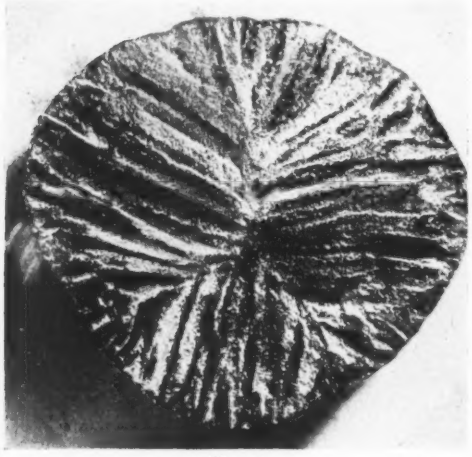

FIG 2

CAST LEAD × 2

As cast the material has radial columnar growth. The photograph shows how the surface has deformed in a like manner.

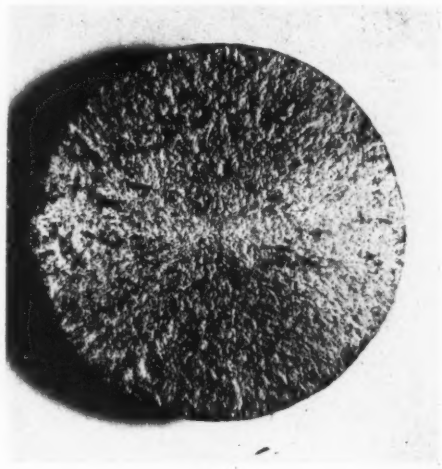

FIG 3

RECRYSTALLIZED LEAD × 2

The cast structure was refined by cold working. The photograph shows how the surface deformation has reacted to the grain refinement.

FIGS 1–3

SHOWING SURFACE DETERIORATION OF ORIGINALLY POLISHED COMPRESSION SPECIMENS AFTER DEFORMATION WITH A VISCOUS LUBRICANT AT THE DIE SPECIMEN INTERFACE

Lubricant viscosity—756 cP at 100° F.

could be achieved whilst the film was still of finite thickness, such that the total load supported was sufficient to initiate bulk plastic deformation of the specimen. In this simple case the assumption was made that the fluid viscosity was independent of pressure.

The analysis has been extended allowing for a reasonable pressure–viscosity characteristic of the interposed fluid. The results support the previous findings and reveal that where the fluid viscosity is pressure-dependent, continuous film conditions may be even more easily achieved than had previously been shown. This analysis is carried out on the assumption that the approaching faces remain flat and parallel to each other, and inferences are made regarding the limiting film thickness at which the maximum pressure reaches an infinitely high value. Obviously the physical assumptions of faces remaining parallel are at this stage untenable, for a normal material, with elastic and plastic properties, and thus from the inference that the progressive build-up of fluid pressure will cause elastic and plastic deformation, leading to dishing of one of the approaching faces. A further analysis is completed on the basis of profiled faces.

The problem is considered not as one involving continuous deformation, but by considering the pressure distributions at some stage after initial deformation has occurred, giving the assumed non-parallel face configuration. It is seen that the distri-

butions remain such that the perpetuation of a dished contour is ensured, providing a reservoir for the establishment of a mechanically trapped film.

ASSUMPTIONS

(1) The usual assumptions of lubrication theory are made that in the equations of motion the inertia and density terms can be neglected by comparison with the viscous terms.

(2) The fluid is considered to behave throughout as a Newtonian fluid.

(3) The fluid viscosity may be a function of the pressure such that:

$$\eta = \eta_0 e^{mp}$$

(4) In the derivation of the expressions for pressure distributions the surfaces remain rigid throughout, retaining the profiles specified.

(5) All thermal effects are neglected.

(6) The fluid is assumed incompressible.

THEORETICAL

It follows from the work of Reynolds [1] that if two surfaces approach each other at a velocity V (the relative velocities in the transverse directions being zero), and the intervening space is occupied by a viscous fluid, then the equation

$$\frac{\partial}{\partial x}\left(\frac{h^3}{\eta}\cdot\frac{\partial p}{\partial x}\right)+\frac{\partial}{\partial y}\left(\frac{h^3}{\eta}\cdot\frac{\partial p}{\partial y}\right)=-12V \quad . \quad (1)$$

relates for a Newtonian fluid the pressure distribution in the film, the instantaneous film thickness, the fluid viscosity, and the relative velocity of approach.

Several conditions may be envisaged leading either to simplification or complication of equation (1).

η may be assumed constant.

h may be assumed constant, *i.e.* approaching flat and parallel surfaces.

η may be assumed a function of fluid pressure, a reasonable assumption being $\eta = \eta_0 e^{mp}$.

h may be assumed variable, *i.e.* h is a function of x and y.

If the approaching bodies are cylindrical in shape, with the cylinder axes in line during approach, equation (1) can be rewritten in cylindrical polar co-ordinates becoming

$$\frac{\partial}{\partial r}\left(\frac{h^3}{\eta}\cdot\frac{\partial p}{\partial r}\right)+\frac{h^3}{r\eta}\cdot\frac{\partial p}{\partial r}+\frac{1}{r}\cdot\frac{\partial}{\partial\theta}\left(\frac{h^3}{r\eta}\cdot\frac{\partial p}{\partial\theta}\right)=-12V \quad . \quad . \quad . \quad (2)$$

which for axial symmetry reduces to

$$\frac{\partial}{\partial r}\left(\frac{h^3}{\eta}\cdot\frac{\partial p}{\partial r}\right)+\frac{h^3}{r\eta}\cdot\frac{\partial p}{\partial r}=-12V$$

i.e.

$$\frac{1}{r}\cdot\frac{\partial r}{\partial r}\left(\frac{rh^3}{\eta}\cdot\frac{\partial p}{\partial r}\right)=12V \quad . \quad . \quad (3)$$

Equation (3) integrates to give

$$r\cdot\frac{\partial r}{\partial p}=-\frac{h^3}{6\eta V} \quad . \quad . \quad . \quad . \quad (4)$$

Various combinations of h and η quoted above when substituted in equation (4) give the normal pressure distributions for the different conditions envisaged.

SOLUTIONS OF THE PARTICULAR CASES

(A) *Fluid Viscosity Dependent on Pressure* ($\eta = \eta_0 e^{mp}$) *Approaching Faces Flat and Parallel* (instantaneous gap $= h_1$)

From equation (4)

$$r\cdot\frac{dr}{dp}=-\frac{{h_1}^3}{6V\eta_0}\cdot e^{-mp}$$

integrates to

$$\frac{r^2}{2}=\frac{{h_1}^3}{6V\eta_0 m}\cdot e^{-mp}+\text{constant}$$

and using the boundary condition that $p = 0$ when $r = R$

$$p_1=-\frac{1}{m}\ln\left\{1-\frac{mk}{4}(R^2-r^2)\right\} \quad . \quad . \quad (5)$$

It is here appropriate to set a value for the viscosity index m. A survey of the ASME pressure viscosity project [9] shows that for paraffinic base lubricants the assumed characteristic $\eta = \eta_0 e^{mp}$ is a reasonable one, where the value of m can be considered constant at $1{\cdot}325 \times 10^{-4}$ in^2/lb over a wide range of pressures and initial viscosities.

Equation (5) shows that

$$p_{1\max}=-\frac{1}{m}\ln\left(1-\frac{mk}{4}R^2\right) \quad \text{at } r=0 \quad (6)$$

giving a limiting value of

$$k_{\text{limit}}\left(=\frac{12V\eta_0}{{h_1}^3}\right)=\frac{4}{mR^2} \quad . \quad . \quad . \quad (7)$$

at which the peak pressure becomes infinite.

Thus, for disks of any given radius R, a limit is set on the parameter $\dfrac{12V\eta_0}{{h_1}^3}$ after which no raidal flow of lubricant can take place, the peak pressure here reaching an infinite value.

Fig 5 shows graphically the values of k_{limit} plotted against R for the accepted value of m.

Equation (7) shows the manner of variation of the limiting film thickness ($h_{1\text{limit}}$) with V, η_0, and R. For a given approach velocity and initial viscosity the value of k approaches its limit as the film thins, and $h_{1\text{limit}}$ coincides with k_{limit}, giving

$$h_{1\text{limit}}=(3m)^{\frac{1}{3}}V^{\frac{1}{3}}\eta_0^{\frac{1}{3}}R^{\frac{2}{3}} \quad . \quad . \quad (8)$$

Equation (8) shows that increasing approach velocity, initial viscosity, and radius all contribute to

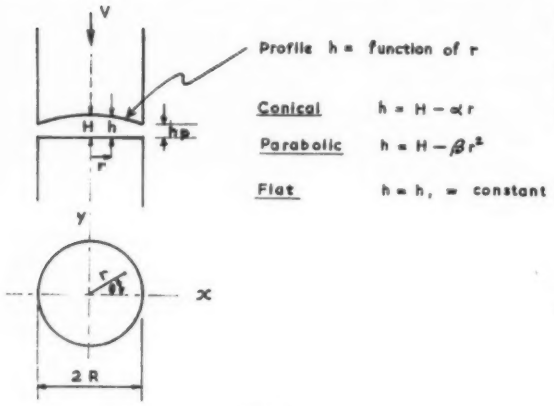

FIG 4
GEOMETRICAL CONFIGURATION

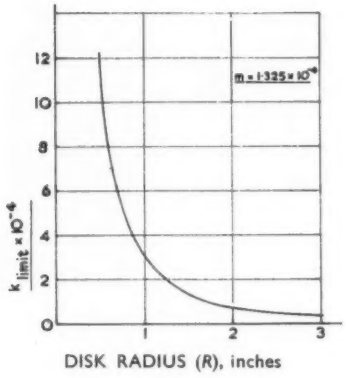

FIG 5
k_{limit} V. DISK RADIUS (R)—CASE (A)

raising the value of h_{1limit}, and if h_{1limit} is calculated for a given set of conditions, revised values resulting from variation of conditions may be obtained direct from equation (8).

It is convenient to continue after assigning specific values to R and V. Since the phenomena of surface deterioration were observed on compression specimens of 1 inch diameter at low rates of strain, comparable values are here taken, namely, $R = 0{\cdot}5$ inch and $V = 1$ inch/min.

(a) *Variation of* h_{1limit} *with initial viscosity* (η_0) ($R = 0{\cdot}5$ inch, $V = 1$ inch/min).

Equation (8), evaluated over a range of initial viscosities zero to 1000 cP, leads to Fig 6, showing the values of h_{1limit} against η_0. From this it is evident that over a considerable range of initial viscosities the limiting film thickness is reached at finite values of h_1 between 0·0001 and 0·0006 inch.

An example can be taken to illustrate the effect of variation of R and V. From Fig 6 $h_{1limit} \simeq 0{\cdot}0005$ inch when $\eta_0 = 500$ cP, $R = 0{\cdot}5$ inch, and $V = 1$ inch/min. If R and V are increased to 2 inches and 5 inches/min respectively, equation (8) shows immediately that

$$h_{1limit} = 0{\cdot}00215 \text{ inch}$$

(b) *Comparison of Maximum Pressures*

(1) Where $\eta_i = \eta_0 e^{mp}$.
(2) Where $\eta_i = \eta_0 =$ constant (*i.e.* $m = 0$).

To illustrate the effect of the pressure–viscosity dependence by comparison with a fluid whose viscosity

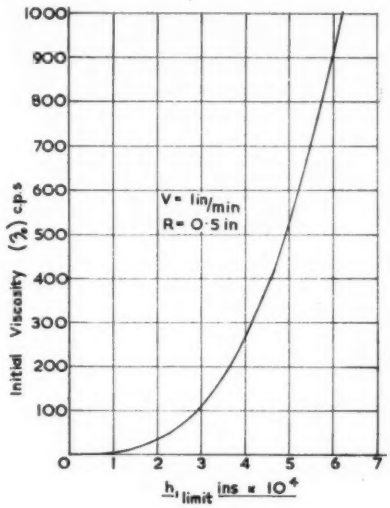

FIG 6
h_{1limit} V. INITIAL VISCOSITY (3)—CASE (A)

is assumed constant, it is necessary in the foregoing analysis only to assume $m = 0$ to give the constant viscosity condition.

It has been shown in equation (6) that

$$p_{1max} = -\frac{1}{m} \ln \left(1 - \frac{mk}{4} R^2\right)$$

On expansion and substitution of $m = 0$, this gives for a constant viscosity fluid

$$p_{2max} = \frac{kR^2}{4} \quad . \quad . \quad . \quad . \quad (9)$$

In the case of $R = 0{\cdot}5$ inch, equation (7) gives

$$k_{limit} = \frac{4}{mR^2} = 12{\cdot}08 \times 10^4$$

the value at which p_{1max} goes to infinity.

A plot of p_{1max} and p_{2max} against values of k up to $12{\cdot}08 \times 10^4$ therefore shows the effect on the peak pressure resulting from the pressure–viscosity de-

pendence. Fig 7 illustrates the rapid increase of p_{1max} as k_{limit} is approached.

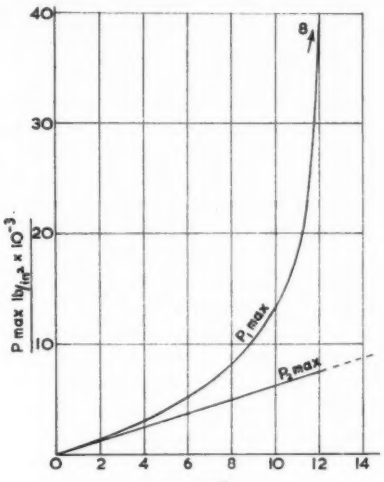

FIG 7

$\frac{p_{1max}}{p_{2max}}$ v. k—CASE (A)

(c) *Comparison of Pressure Distributions*

(1) Where $\eta_i = \eta_{i0}e^{mp}$.
(2) Where $\eta_i = \eta_{i0}$ = constant (*i.e.* $m = 0$).

Equation (5) gives the expression for p_1 and substitution of $m = 0$ leads to

$$p_2 = \frac{k}{4}(R^2 - r^2) \quad . \quad . \quad . \quad (10)$$

an expression previously used by Needs [8] in connexion with a disk viscometer.

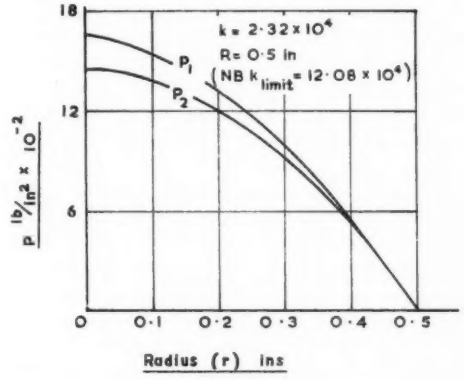

FIG 8

PRESSURE DISTRIBUTIONS—CASE (A)

Again for a value of $R = 0{\cdot}5$ inch, the pressure distributions for various values of k up to $k_{limit} = 12{\cdot}08 \times 10^4$ are shown in Figs 8–10. As expected, at low values of k, where maximum pressures are low, there is little divergence of p_1 from the parabolic profile of p_2, but with increasing k considerable divergence occurs.

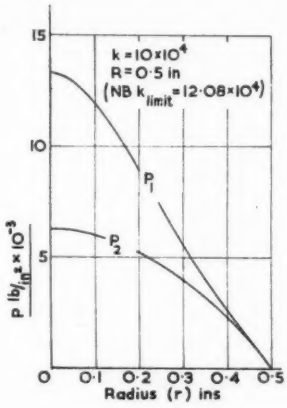

FIG 9

PRESSURE DISTRIBUTIONS—CASE (A)

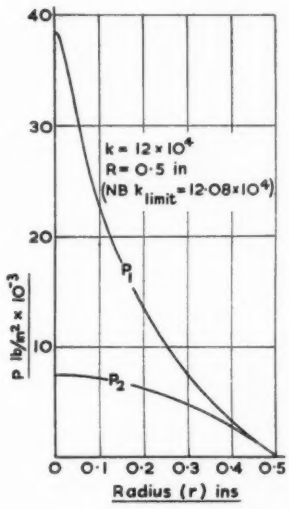

FIG 10

PRESSURE DISTRIBUTIONS—CASE (A)

(d) *Comparison of Total Supported Loads and Mean Pressures*

(1) Where $\eta_i = \eta_{i0}e^{mp}$.
(2) Where $\eta_i = \eta_{i0}$ = constant (*i.e.* $m = 0$).

If the pressure distribution is known as a function of r, then the total supported load

$$W = \int_0^R 2\pi rp \, . \, dr \quad . \quad . \quad . \quad (11)$$

and the mean pressure

$$\bar{p} = W/\pi R^2$$

It follows by substitution of p_1 and p_2 in equation (11) that

$$W_1 = \frac{\pi R^2}{m} - \frac{\pi R^2}{m} \ln\left(1 - \frac{mkR^2}{4}\right) + \frac{4\pi}{m^2 k} \cdot \ln\left(1 - \frac{mkR^2}{4}\right) \quad (12)$$

$$W_2 = \pi k R^4/8 \; . \; . \; . \; . \quad (13)$$

$$\bar{p}_1 = \frac{1}{m} - \frac{1}{m} \ln\left(1 - \frac{mkR^2}{4}\right) + \frac{4}{m^2 k R^2} \ln\left(1 - \frac{mkR^2}{4}\right) \quad (14)$$

and

$$\bar{p}_2 = \frac{kR^2}{8} \; . \; . \; . \; . \; . \quad (15)$$

For $R = 0{\cdot}5$ inch (*i.e.* $k_{\text{limit}} = 12{\cdot}08 \times 10^4$), the plot shown in Fig 11 of W_1 and W_2 (or $\bar{p}_1$ and $\bar{p}_2$) against k, up to its limiting value, illustrates again the appreciable influence of the pressure–viscosity dependence at high values of k.

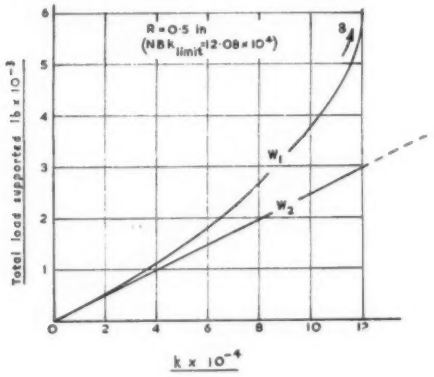

FIG 11

TOTAL LOAD SUPPORTED v. k—CASE (A)

It is relevant here to quote an example, assuming constant viscosity, which illustrates that a total load may be supported through a continuous film, sufficient to initiate plastic yielding of a metallic specimen.

It has been shown previously [7] that for disks of 1 inch diameter, approaching at 1 inch/min in the presence of a fluid of constant viscosity 100 cP, a total load of 35,000 lb can be supported when the film reduces to 0·000126 inch. Similarly a 1000-lb load can be supported through a film of thickness 0·000414 inch.

These two cases are taken since 35,000 lb and 1000 lb are the approximate total loads required to reach the yield point of 1-inch diameter specimens in mild steel and lead respectively. Whilst it is appreciated that elastic and local plastic deformation will occur before the yield load is reached, with the consequence that the faces are no longer parallel, the simplified example does indicate the possibility of deformation commencing in the presence of continuous films of thickness greater than the normal surface roughness measurements (asperity heights) of engineering surfaces.

Implications of the Foregoing Analysis

The foregoing analysis has been carried out in an attempt to justify the assumption that during the approach of a compression pad towards the surface of a lubricated compression specimen a pressure distribution in the fluid film might be established such that the initial surface deformation would occur mainly via a fluid film. This would provide a satisfactory explanation for the unusual surface appearances observed experimentally after deformation, which indicate the absence of metal to metal contact.

It is shown that in the case of a fluid of constant viscosity, total loads of considerable magnitude may be supported in the fluid film whilst it is finite in thickness. The load approaches infinity, however, only in the limit where the film thickness approaches zero.

On the other hand, when the pressure–viscosity characteristic is incorporated, the significant fact emerges that for a specimen of a given radius a limiting value of the parameter

$$k\left(= \frac{12 V \eta_0}{h_1^3}\right) = \frac{4}{mR^2}$$

is reached at which the maximum pressure, mean pressure, and supported load become infinite. The consequence is that, for a given disk radius, velocity of approach, and initial viscosity a limiting film thickness is achieved beyond which no further expulsion of the lubricant can theoretically occur. The various figures and relationships quoted enable the value of limiting film thickness to be evaluated readily for any given operating conditions, and again it is apparent that appreciable limiting film thicknesses result from quite moderate operating circumstances. This aspect has been discussed at some length, since it illustrates clearly the well-marked consequences of using a fluid where viscosity is pressure dependent.

The inadequacies of the analysis so far in its application to the lubricated compression test are, however, obvious in view of the assumptions made that the approaching surfaces remain flat and parallel and that they continue to approach at constant velocity. Once deformation of one of the members occurs, the physical assumptions made are untenable and the pressure distribution will be modified. However, the analysis is acceptable as the surfaces approach prior to the start of deformation, when an initial pressure distribution (near parabolic) as described is set up, until such time as elastic, followed by plastic, deformation of one of the members occurs.

The implication here is that the deforming surface will take on a dished contour, and it is of further

interest to examine what modifications to the pressure distribution result from such circumstances.

Thus, in what follows the cases are taken where it has been assumed that at some instant of the compression process, whilst the approaching pad remains flat and rigid the deforming surface has assumed a profile, radially symmetrical, but with a central depression. Two such profiles are taken, one conical and one parabolic, and the pressure distributions calculated, in both cases with the assumption of a constant viscosity fluid, and in the latter case also with a fluid whose viscosity is pressure dependent.

(B) *Fluid Viscosity Independent of Pressure* ($m = 0$, *i.e.* $\tau_i = \tau_0$)

One Approaching Face Flat

One Approaching Face Conically Recessed

For a shallow symmetrical conical profile the gap between the approaching surfaces is defined by

$$h = H - \alpha r \quad . \quad . \quad . \quad . \quad (16)$$

where H is the instantaneous maximum gap and α the inclination of the profile to the flat face.

Substituting equation (16) in equation (4) gives

$$\int \frac{r \, . \, dr}{(H - \alpha r)^3} = -\frac{p}{6\tau_0 V} + \text{constant}$$

which, with the boundary condition $p = 0$ at $r = R$ (as long as $H > \alpha R$), leads to

$$\frac{p_3}{3\tau_0 V} = \frac{H(R^2 - r^2) - 2\alpha R r(R - r)}{(H - \alpha R)^2(H - \alpha r)^2} \quad . \quad (17)$$

The maximum pressure occurs still at $r = 0$ giving

$$p_{3\max} = \frac{3\tau_0 V R^2}{H(H - \alpha R)^2} \quad . \quad . \quad (18)$$

which shows that $p_{3\max}$ approaches infinity only as αR approaches H, *i.e.* as the peripheral gap closes.

Equations (17) and (18) both show that the pressures in the film increase both with decrease of the gap and with decrease of the cone angle α.

If equation (18) is expressed in terms of the peripheral gap h_p, then since

$$h_p = H - \alpha R$$

$$p_{3\max} = \frac{3\tau_0 V R^2}{(h_p + \alpha R)h_p^2} \quad . \quad . \quad (18a)$$

showing that for a given peripheral gap, decrease of α leads to an increase of $p_{3\max}$, or alternatively, for a given value of α decrease of h_p affects $p_{3\max}$ similarly.

(C) *Fluid Viscosity Dependent on Pressure* ($\tau_i = \tau_0 e^{mp}$)

One Approaching Face Flat

One Approaching Face Parabolically Recessed

For a symmetrical parabolic profile the gap between the approaching surfaces is defined by

$$h = H - \beta r^2 \quad . \quad . \quad . \quad . \quad (19)$$

which, substituted in equation (4) with the boundary condition that $p = 0$ at $r = R$ (as long as $H > \beta R^2$), leads to the solution

$$p_4 = -\frac{1}{m} \ln . \frac{3\tau_0 m V}{2\beta} \left\{ \frac{(H - \beta R^2)^2 - (H - \beta r^2)^2}{(H - \beta r^2)^2 (H - \beta R^2)^2} + \frac{2\beta}{3\tau_0 m V} \right\} \quad . \quad . \quad (20)$$

$p_{4\max}$ still occurs at $r = 0$, giving

$$p_{4\max} = -\frac{1}{m} \ln \left\{ 1 - \frac{3\tau_0 m V}{2} \cdot \frac{R^2(2H - \beta R^2)}{H^2(H - \beta R^2)^2} \right\} \quad (21)$$

Here now a limiting film thickness is reached at which $p_{4\max}$ becomes infinity before the peripheral gap closes, this thickness occurring when a suitable value of H satisfies

$$3\tau_0 m V R^2(2H - \beta R^2) = 2H^2(H - \beta R^2)^2 \quad (22)$$

Thus, as is shown subsequently in a specific case, this configuration, when used in conjunction with a fluid with a pressure–viscosity characteristic, enables a theoretically infinite value of $p_{4\max}$ to occur before closure of the peripheral gap.

If in this case m is assumed zero, the solution is obtained for the same geometrical configuration, but with a fluid of constant viscosity. From equations (20) and (21) the pressure distribution and maximum pressure become

$$\frac{2}{3\tau_0 V} \cdot p_5 = \frac{(H - \beta r^2)^2 - (H - \beta R^2)^2}{\beta(H - \beta R^2)^2(H - \beta r^2)^2} \quad . \quad (23)$$

and

$$p_{5\max} = \frac{3}{2} \cdot \tau_0 V \cdot \frac{R^2(2H - \beta R^2)}{H^2(H - \beta R^2)^2} \quad . \quad (24)$$

Equation (24) shows, as in the other cases for a constant viscosity fluid, that the maximum pressure approaches infinity only as the peripheral gap closes.

Comparison of Pressure Distributions for all Cases

The pressure distributions p_1, p_2, p_3, p_4, and p_5 in terms of radius are given by equations (5), (10), (17), (20), and (23), for the various combinations of gap profile and varying or constant viscosity. It is of interest to compare these distributions under a given set of approach conditions.

Section (A) shows that for approaching parallel faces the value of k_{limit} is reached at $12{\cdot}08 \times 10^4$ when the viscosity function is

$$\tau_i = \tau_0 e^{1{\cdot}325 \times 10^{-4} \cdot p}$$

In addition we have the pressure profiles p_1 and p_2 plotted (Fig 10) for a value of $k = 12 \times 10^4$, and disks of diameter 1 inch (*i.e.* $R = 0{\cdot}5$ inch). Thus it is

convenient to use these values in determining the full set of distributions. To give $k\left(=\frac{12V\eta_0}{h_1^3}\right)$ a value of 12×10^4 appropriate values of h_1, η_0, and V are:

$h_1 = 0{\cdot}0003$ inch
$\eta_0 = 100$ cP
$V = 1{\cdot}12$ inch/min

where it must be remembered that h_1 is the instantaneous (but constant) gap in the case of parallel, flat, approaching faces. Fig 12 re-plots the values of p_1 and p_2 from Fig 10.

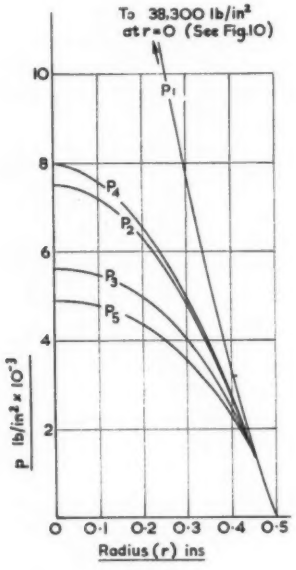

FIG 12

PRESSURE DISTRIBUTIONS—CASES (A), (B), AND (C)

$R = 0{\cdot}5$ inch: $V = 1{\cdot}12$ inch/min: $\eta_0 = 100$ cP
Minimum gap in all cases = 0·0003 inch

p_1—Parallel faces	$\eta = \eta_0 e^{mp}$
p_2—Parallel faces	$\eta = \eta_0 =$ constant
p_3—Conical profile	$\eta = \eta_0 =$ constant, $\alpha = 0{\cdot}0002$
p_4—Parabolic profile	$\eta = \eta_0 3^{mp}$, $\beta = 0{\cdot}0004$
p_5—Parabolic profile	$\eta = \eta_0 =$ constant, $\beta = 0{\cdot}0004$

To establish comparable circumstances in the case of profiled faces, it is assumed that the peripheral radii (R), the initial fluid viscosity (η_0), and the approach velocity (V) remain at the values given above, and that the peripheral gap h_p is the same (0·0003 inch) as the above quoted figure for h_1. However, since the profiles are depressed, a maximum gap (H) must be assumed, and this is taken to be 0·0004 inch. The small difference between h_p and H is set deliberately, as it is considered in practical cases to be quite sufficient to be in excess of the normal surface roughnesses likely to be encountered.

It follows that for the conical profile, since $H = h_p + \alpha R$,

$$\alpha = 0{\cdot}0002$$

and for the parabolic, since $H = h_p + \beta R^2$

$$\beta = 0{\cdot}0004$$

Substitution of the above values where appropriate in the expressions for p_3, p_4, and p_5 enables the pressure distributions to be compared in all the cases taken. These are given in Fig 12, and show that whereas p_1 is tending to a high (38,000 psi) central value, the introduction of profiled faces reduces that value. The parabolic profile, p_5, shows a pressure distribution slightly lower than that of the conical face p_3 with a constant viscosity fluid, but the incorporation of a pressure–viscosity characteristic shows the anticipated rise in pressure distribution to p_4.

It has been shown in equation (22) that a limiting film thickness exists when $p_{4\max}$ becomes infinite. In the present case $p_{4\max}$ has been shown (Fig 12) to be 8000 psi when the maximum gap H is 0·0004 inch. Graphical solution of equation (22) shows that this is approaching the limit, which in fact occurs when H is approximately 0·00037 inch.

DISCUSSION

The limitations of the analysis resulting from its treatment as an incremental as opposed to a continuous deformation process are appreciated and accepted. It is doubtful, however, whether the complications involved in extending the elasto-hydrodynamic problem to the plastic range justify further work at present. Indeed, the problem itself is basically different from the normal elasto-hydrodynamic one. This latter is a problem in which once the task of satisfying the elastic and hydrodynamic equations simultaneously has been accomplished, the deformed surfaces retain the same profiles for a given set of operating conditions. The present problem is one in which the two surfaces are continuously approaching whilst simultaneously one of them is continuously deforming. For a full solution,* therefore, it would appear that another variable (time) should be incorporated. This would allow (dh/dt) for the time variation of the gap at any radial position due to the plastic deformation, superimposed upon the constant approach velocity assumed.

However, since experimental evidence [6, 7] indicates the presence of a continuous film (whose thickness need not be greatly in excess of the normal surface roughness encountered), some analytical justification for its presence is desirable. It is considered that by

* See Appendix for a simplified approach to the plastic problem.

inference from the incremental procedure here adopted, the film presence may be satisfactorily explained.

If the two faces are assumed flat and parallel on initial approach and the fluid viscosity is pressure dependent, the initial approach stimulates a pressure distribution (p_1) as defined in equation (5). Such a distribution would reasonably cause the deforming face to assume a dished profile.[5] In so doing, the pressure distribution would itself be subject to change as a result of:

(*a*) the changing deformed profile, and
(*b*) the now non-constant velocity of approach at adjacent positions of the mating faces.

However, once dishing has occurred, further approach on an incremental basis between the now non-parallel faces leads to a pressure distribution such as that described for example in Case (C) of the foregoing. Here the pressure still reaches its maximum value along the central axis, and theoretically a limiting film thickness occurs where this pressure becomes infinite. Thus, although the progressive deformation leads to a constantly varying pressure distribution, conditions are such that the hydrodynamic effect, especially where the fluid viscosity is pressure dependent, having once established a depressed contour is likely to maintain it until such time as metal to metal contact is made. This will initially be at the peripheral radius, explaining the presence of the observed bright annular peripheral contact ring. Beyond this stage the hydrodynamic effect is of minor importance as mechanical entrapment of the film is ensured. Further deformation builds up hydrostatic film pressure with the minimum of intermetallic contact. This allows preferential distortion of the grains until such time as lateral expansion thins the film, and random grain distortion disrupts the surface to an extent where discrete contact areas begin to appear.

Although this effect has previously been demonstrated experimentally on a microscopic scale,[6, 7] an attempt to demonstrate it on a macroscopic scale is worthy of mention.

A simple experiment was conducted on a mild steel compression specimen 1 inch long by 1 inch diameter with a polished flat contact end.

In place of a lubricant, a $\frac{1}{16}$-inch thick sheet of rubber (which exhibits hydrostatic characteristics) was interposed between the specimen and the die. The die was then loaded on at approximately 4 inches/min, the operation being stopped when the specimen length reduced to 0·85 inch. The initial specimen surface profile was measured across two diameters at right angles, as shown in Fig 13, which shows it to have been slightly crowned. After compression a noticeable dish had formed, the contour of which is plotted in Fig 14. Figs 15 and 16 show the effect photographically, and show clearly how the originally polished surface has assumed a microscopically roughened appearance in the absence of metallic contact. This effect is identical to that seen in Fig 1, where a fluid lubricant was present between the surfaces.*

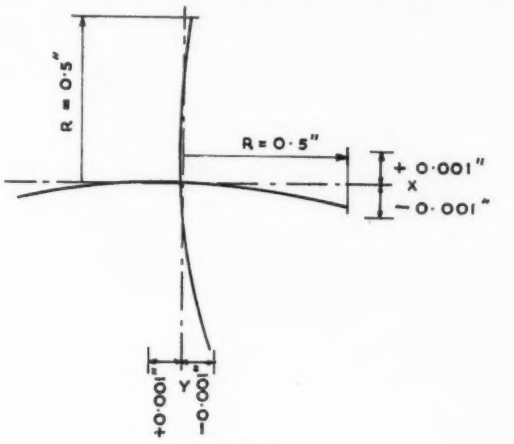

FIG 13
INITIAL PROFILE OF SPECIMEN ACROSS DIAMETERS X AND Y
Specimen slightly crowned.

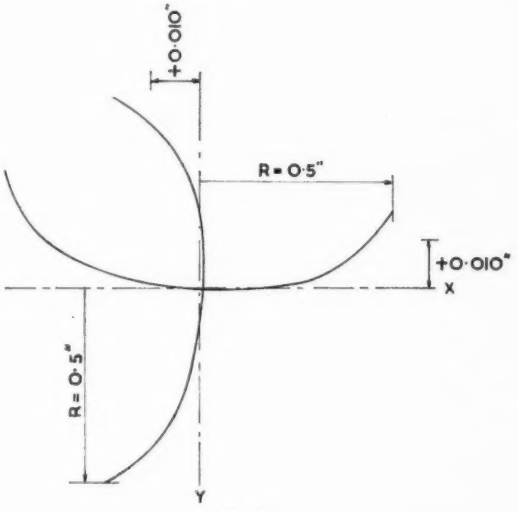

FIG 14
FINAL PROFILE OF SPECIMEN ACROSS DIAMETERS X AND Y
Showing dished profile.

* Since the submission of this paper, some experiments have been conducted on flat-faced, mild steel specimens with fluid lubricants which have produced dished contours of measurable dimensions after plastic deformation. It is hoped to publish the results of these, and other experiments currently being carried out, in the near future.

× 2

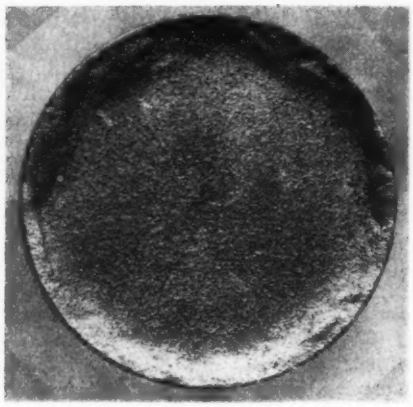

× 2

FIG 15

FIG 16

FIGS 15 AND 16

SHOWING DISHING AND DETERIORATION OF SPECIMEN CONTACT FACE AFTER DEFORMATION WITH RUBBER "LUBRICANT"

End face originally highly polished. Material annealed mild steel.

ACKNOWLEDGMENTS

The author wishes to thank his colleagues, Dr D. G. Ashwell and Dr D. Rogers, for their interest and assistance, and A. A. Milne for his helpful comments in private communication.

References

[1] Reynolds, O. *Phil. Trans. Roy. Soc., Lond.*, 1886, **177**, 157.
[2] McEwen, E. *J. Inst. Petrol.*, 1952, **38**, 646.
[3] Cameron, A. *J. Inst. Petrol.*, 1952, **38**, 614.
[4] Dowson, D., and Higginson, G. R. *J. Mech. Engng Sci.*, 1959, **1**, 6.
[5] Bowden, F. P., and Tabor, D. "Friction and Lubrication of Solids," Oxford: Clarendon Press, 1950.
[6] Butler, L. H. *Metallurgia, Mchr*, in process of publication.
[7] Butler, L. H. *J. Inst. Metals*, in process of publication.
[8] Needs, S. J. *Trans. Amer. Soc. mech. Engng*, 1940, **62**, 331.
[9] ASME. Pressure Viscosity Report, 1953 (2 vols).

APPENDIX

Pressure Distribution Allowing for the Recession of the Deforming Surface

In the foregoing, allowance has been made for the fact that the approaching surfaces may be non-parallel. In each case, however, the solution for pressure distribution has been made on the assumption that the deformed surface is instantaneously at rest. This would not be the case in the later stages of approach, when the deformed profile would itself be receding from the die with a velocity varying across the diameter.

It is proposed here to investigate analytically such a case in which

(*a*) the instantaneous gap may be defined as $h^3 = f(r)$;
(*b*) the die approach velocity is constant $= V$;
(*c*) the viscosity of the fluid may vary with pressure, $\eta = \eta_0 e^{mp}$;
(*d*) the velocity of recess of the deforming surface may be expressed as a function of r at the instant considered

i.e. $$v = \psi(r) \quad . \quad . \quad . \quad . \quad . \quad \text{A(1)}$$

Under these conditions,

velocity of approach at radius $r = V - v = V - \psi(r)$ A(2)

$\therefore$ volume of fluid displaced at element/unit time $= 2\pi r\, dr[V - \psi(r)]$ A(3)

$\therefore$ total volume displaced unit/time up to radius $r =$

$$\int 2\pi r[V - \psi(r)]dr \quad \text{A(4)}$$

$\therefore$ it follows from continuity of flow that

$$\int r[V - \psi(r)]dr = -\frac{r \cdot f(r)}{12\eta} \cdot \frac{dp}{dr} \quad . \quad . \quad \text{A(5)}$$

i.e. $$\int r[V - \psi(r)]dr = -\frac{rh^3}{12\eta_0} \cdot e^{-mp} \cdot \frac{dp}{dr} \quad . \quad \text{A(6)}$$

With the knowledge (assumed) of $\psi(r)$ equation A(6) may be solved with more or less computational effort, depending upon the complexity of the expressions for $\psi(r)$ and h^3, and whether the pressure–viscosity characteristic is allowed for. For illustration a relatively simple case is taken where:

(*a*) The deforming profile is conical, *i.e.* the instantaneous gap is defined by

$$h = H - \alpha r$$

(*b*) The die approach velocity is V.
(*c*) The fluid viscosity is independent of pressure, *i.e.* $\eta = \eta_0$.
(*d*) The deforming profile is receding with a velocity distribution instantaneously linear along a radius, varying from aV at the axis to bV at the periphery.

Thus

$$v = \psi(r) = Va - V(a - b)r/R \quad . \quad . \quad . \quad \text{A(7)}$$
$$V - \psi(r) = V(1 - a) + V(a - b)r/R \quad . \quad \text{A(8)}$$

and $$\int r[V - \psi(r)]dr = \frac{Vr^2(1-a)}{2} + \frac{V}{3}\cdot\frac{(a-b)}{R}\cdot r^3 \quad \text{A(9)}$$

and from equation A(6)

$$-\frac{h^3}{12\eta_0}\cdot\frac{dp}{dr} = \frac{V}{2}(1-a)r + \frac{V}{3}\frac{(a-b)}{R}\cdot r^2 \quad . \quad \text{A(10)}$$

$$\therefore \; -\frac{p}{6\eta_0 V} + C = \int\frac{(1-a)r}{(H-\alpha r)^3}\cdot dr + \int\frac{2}{3}\cdot\frac{(a-b)}{R}\cdot\frac{r^2}{(H-\alpha r)^3}\cdot dr$$

which upon integration yields

$$-\frac{p}{6\eta_0 V} = \frac{(1-a)}{\alpha^2}\left[\frac{H}{2(H-\alpha r)^2} - \frac{H}{2(H-\alpha R)^2} - \frac{1}{(H-\alpha r)} + \frac{1}{(H-\alpha R)}\right] + \frac{(a-b)}{3\alpha^3 R}\left[\frac{H^2}{(H-\alpha r)^2} - \frac{H^2}{(H-\alpha R)^2} - \frac{4H}{(H-\alpha r)} + \frac{4H}{(H-\alpha R)} + 2\ln\frac{(H-\alpha R)}{(H-\alpha r)}\right] \quad \text{A(11)}$$

giving the pressure distribution in the case considered. When $a = b = 0$ equation A(11) reduces to the appropriate previous Case (B).

In a realistic case in which $b < a < 1$ equation A(10) shows $\frac{dp}{dr}$ to be always negative, and equal to zero at $r = 0$. Thus again the pressure distribution is such as to retain a pressure profile with a central maximum value, and the previous inference of perpetuation of the dished profile is further confirmed.

The general problem is, of course, one of far greater complexity than has been currently considered. Compatibility must be achieved between the equations governing the generation of fluid pressure, and the plastic deformation of the surfaces, allowance being made simultaneously for the fact that the surface profile is continuously changing. It seems unlikely that anything other than a numerical solution might be achieved. The present work suggests, however, that an approach on an incremental basis followed by a simplified dynamic analysis may yield useful results in applications where loading is sufficiently severe to cause plastic deformation.

SOUTH AFRICAN SHALE-OIL BITUMEN AS A ROAD BINDER*

By E. J. DICKINSON†

SUMMARY

Although South African shale-oil bitumen has been used as the binder for road wearing courses with some success, carefully controlled road experiments have shown that this bitumen is less durable than certain petroleum bitumens and fluxed lake asphalt from Trinidad, but, in certain constructions, slightly more durable than some locally produced road tars of coke-oven origin.

Laboratory examination of the physical and chemical properties of the bitumen indicated that its inferior durability is due primarily to its higher temperature susceptibility of viscosity and its tendency to become brittle at low road temperatures and also to its high susceptibility to chemical attack by atmospheric oxygen.

Chemical investigations on the mechanism of the reaction of oxygen with the bitumen indicated that the main reaction is with hydrocarbon constituents of the bitumen, and particularly with some of the unsaturated hydrocarbons present. Dehydrogenation and condensation take place, and high molecular weight hydrocarbons, which increase the viscosity of the bitumen, are formed.

Sulphation of the unsaturated hydrocarbons by low-temperature treatment with dilute sulphuric acid, although reducing the susceptibility of the bitumen to oxidation, gave a product which decomposed when heated to normal bitumen handling temperatures. No practical method for overcoming this difficulty was found.

INTRODUCTION

South African shale-oil, produced by the low-temperature retorting of torbanite, has been processed for the production of bituminous road binders since 1938, and the bitumens obtained have given satisfactory performance both in pre-mix and surface dressing road constructions.

Robertson [1] had described the general properties of the crude shale oil and the method of processing to obtain motor spirit and bitumen as the main products. Briefly, the crude oil is subjected to a combined reforming and distillation process to give a 100–200-pen bitumen as the distillation residue. Lime is injected into the gas oil stream of the plant at the quench point to reduce corrosion by sulphur compounds and remains in the bitumen distillation residue. The bitumen is used for road purposes either without further treatment or cut back with kerosine or naphtha fractions obtained from the distillation unit of the processing plant.

Production of the shale oil has been decreasing since 1956, and will probably cease altogether within the near future.

Although the bitumen had, for many years, been successfully used for road surfacing, it was not until 1951 that a systematic attempt was made to assess the quality of the material as a road binder and to compare its road performance with that of petroleum bitumens. This investigation was undertaken by the Bituminous Binder Research Unit of the South African Council for Scientific and Industrial Research, the South African Torbanite Mining and Refining Company Ltd being one of the sponsors of the Unit.

The factors affecting the performance of a bituminous binder in a road surfacing are so complex that, as yet, no tests have been devised to predict with absolute certainty the comparative performance of different binders in use. At the outset of the investigation, therefore, several carefully controlled road experiments were laid to compare the performance of the shale-oil bitumen with petroleum bitumens and with locally produced tars of coke-oven origin in both single re-seal maintenance work and pre-mix construction. The oldest of the road experiments has now been laid for seven years, and there is sufficient information from these and some of the younger experiments to give an assessment of the relative performance of the binders in the different types of construction.

COMPARATIVE ROAD PERFORMANCE OF SHALE-OIL BITUMEN, PETROLEUM BITUMENS, AND TARS OF COKE-OVEN ORIGIN

(1) *For Re-sealing Existing Bituminous Roads*

Three road experiments were laid to compare the performance of the different types of binder in the single surface treatment of existing bituminous roads. In every case the binders were tested at three or four different rates of application for each binder–stone combination, and special precautions were taken to ensure that the rate of binder application was even over the whole area of the experimental section. Full information on these road experiments has been published elsewhere.[2]

The experimental sections were inspected at yearly intervals by a panel of at least seven experienced observers and the average assessment of this panel recorded.

From the results of these inspections the lives of the surfacings were determined. Generally the surfacings

* MS received 21 September 1959.

† National Institute for Road Research, South African Council for Scientific and Industrial Research.

deteriorated by loss of stone (fretting), but whenever deterioration took place by "fatting up," this is indicated in the text.

The first experiment was laid on a road carrying approximately 3000 vehicles/day, and the life of the different binder–stone combinations is given in Table I.

TABLE I

Life (in Years) of Experimental Single Surface Treatments Laid on a Road in the Transvaal Carrying 3000 Vehicles/Day.

Type of stone	Dolerite		Quartzite	
Size of stone	½–¼ inch	¾–½ inch	½–¼ inch	¾–½ inch
Binder:				
Shale-oil bitumen (M.C.5 grade)	4	5	4	5
180/200 pen petroleum bitumen (Texan crude source)	Greater than 7	Greater than 7	Greater than 7	Greater than 7
180/200 pen fluxed refined lake asphalt from Trinidad	—	—	7	Greater than 7
Coke-oven tar 45/50 E.V.T.	—	—	3	7

TABLE II

Life (in Years) of Experimental Single Surface Treatments Laid on a Road in the Transvaal Carrying 300 Vehicles/Day

Type of stone	Dolerite			Quartzite		
Size of stone	½–¼ inch	½–¼ inch	¾–½ inch	½–¼ inch	½–¼ inch	¾–½ inch
Binder:						
Shale-oil bitumen (M.C.5 grade)	4	2	1	5	1	1
180/200 pen petroleum bitumen (Texan crude origin)	5 (became fat)	7 (became fat)	Greater than 7	Greater than 7 (becoming fat)	7	Greater than 7
180/200 pen fluxed refined lake asphalt from Trinidad	—	—	—	7	3	5
Coke-oven tar 45/50 E.V.T.	—	—	—	4	Less than 1	1

TABLE III

Life (in Years) of Experimental Single Surface Treatments Laid on a Road in the Cape Province (Karroo) Carrying 50 Vehicles/Day

(Rates of binder application for ½–¼-inch stone were in the range 0·24–0·30 gal/sq yd; Rates of binder application for ¼–$\frac{1}{16}$ inch stone were in the range 0·16–0·20 gal/sq yd)

Size of stone	½–¼ inch	¼–$\frac{1}{16}$ inch
Binder:		
Shale-oil bitumen (M.C.5 grade)	4	Greater than 6½
Shale-oil bitumen (180/200 pen grade)	6½	—
500/700 grade petroleum bitumen of Persian crude origin	Greater than 6½	—
180/200 pen fluxed refined lake asphalt from Trinidad	Greater than 6½	Greater than 6½
Coke-oven tar 45/50 E.V.T.	Less than 1	—

The second experiment was laid on a road carrying approximately 300 vehicles/day at a site close to the first experiment. The lives of the different binder–stone combinations used in this experiment are given in Table II.

The third experiment was laid in a different area from the first two on a road carrying only 50 vehicles/day. Only one type of stone (dolerite) was used.

The life of the surface treatments with the different bitumens used in this experiment is given in Table III.

Results from the single re-seal experiments indicate that the shale-oil bitumen does not give such a good performance in this type of road maintenance as petroleum bitumens or fluxed refined lake asphalt from Trinidad, but in most cases a slightly better performance than the coke-oven tars tested. Of the three types of bitumen, those derived from petroleum have given the best performance.

(2) *Comparative Road Performance in Pre-mix Surfacings*

A comprehensive pre-mix surfacing experiment comparing the performance of several types of bitumen in different pre-mix compositions was laid in 1953 on a road in the Transvaal carrying 1200 vehicles/day. Full details of the experiment, together with road performance results up to five years after laying, have been published elsewhere.[3]

In this experiment binder type, binder content, type of aggregate, and grading of aggregate were systematically varied, and the performance of the experimental sections was assessed yearly by a panel of experienced observers in the same manner as the single surface treatment experiments. Although at this stage it is impossible to assess the relative performance of the binders in terms of the ultimate road life of the experimental sections, some information on this can be deduced from a consideration of the range of binder content with each binder–aggregate combination which is in satisfactory condition after six years on the road. Table IV gives this data.

The information given in Table IV indicates that the shale-oil bitumens do not give such a good performance in pre-mix compositions as the petroleum bitumen and the fluxed refined lake asphalt. The performance of the 180/200 pen grade shale-oil bitumen and the tar are approximately the same. After six years on the road, the only satisfactory compositions with shale-oil bitumen are those with dense and medium aggregate gradings and using the 180/200 pen grade material. Even with this combination the bitumen content range is small compared with the petroleum bitumen, and cracking has taken place in the surfacings with the dense grading. The best compositions with the M.C.5 grade shale-oil bitumen (using medium and dense aggregate gradings with quartzite stone) were satisfactory after four years on the road.

In both single re-seal maintenance and pre-mix construction, therefore, the shale-oil bitumen has been

shown to give an inferior performance to petroleum bitumens, although a properly applied single surface treatment with the shale-oil bitumen could be expected to last four to five years on a medium-trafficked road.

It was realized at the start of the work that the road durability of the shale-oil bitumen was inferior to that of straight-run petroleum bitumens, and a detailed laboratory investigation of the material was begun at an early stage, with the final object of finding ways of improving durability.

In the first place a survey of the physical and chemical properties of the material, relevant to its use as a road binder, was made, and these properties were compared with those of petroleum bitumens and fluxed refined lake asphalt from Trinidad. 180/200 pen grade "straight-run" shale-oil bitumens were mainly studied.

TABLE IV

Binder Content Ranges (% wt of Mixed Materials) for Experimental Pre-mix Surfacings in Satisfactory Condition Six Years After Laying

Type of aggregate	Quartzite	Dolomite	Dolomite	Quartzite	Dolomite	Quartzite	Dolomite
Grading of aggregate * (max size ½-inch):							
% wt passing ½-inch mesh sieve	14	12	24	36	36	52	52
% wt passing No. 200 mesh sieve	6	5	8	9	9	13	10
Binder:							
Shale-oil bitumen (M.C.5 grade)	None	None	None	None	None	None	None
Shale-oil bitumen (180/200 pen grade)	None	None	None	7·5–8·5	None	6·5–8·5 (cracked)	None
180/200 pen grade petroleum bitumen of Trinidad crude origin	3·5–7·5	3·5–8·0	4·0–8·0	4·0–8·5	4·5–7·5	5·0–6·5	4·5–7·5
180/200 pen grade fluxed refined lake asphalt from Trinidad	5·5–7·5	None	None	5·5–8·0	6·0–8·0	5·5–9·0	5·5–8·5
Coke-oven tar 45/50 E.V.T.	None	None	None	None	8·5 only	8·5 only	8·0–10·0

* Determined by analysis of samples of mixed materials (wet sieving).

COMPARISON OF THE PHYSICAL AND CHEMICAL PROPERTIES OF SHALE-OIL AND OTHER BITUMENS

(1) *Standard Road Bitumen Tests for 180/200 pen Grade Materials*

The results of tests on samples of shale-oil bitumen, straight-run petroleum bitumen, and fluxed refined lake asphalt from Trinidad are given in Table V.

TABLE V

Standard Test Results

Bitumen	Shale-oil bitumen	Straight-run Venezuelan bitumen	Straight-run Persian bitumen	Fluxed refined lake asphalt from Trinidad
Penetration at 25° C	181	172	174	176
Softening point (R. & B.), °C	38·9	40·0	40·8	39·4
Solubility in CS_2 (% wt)	97·5	99·2	99·9	84·2
Specific gravity at 25/25° C	1·076	1·016	1·016	1·145
Ductility at 25° C	100+	—	100+	100+
Loss on heating test:				
% loss in wt	0·53	0·27	0·50	0·88
Penetration after heating % of original	61	90	72	88

The standard tests on road bitumens are primarily for controlling manufacture and do not give much information on the performance of the material in use. The results given in Table V do indicate, however, that the shale-oil bitumen has a higher specific gravity and a higher temperature susceptibility of viscosity than the petroleum bitumens, characteristics which would be expected of a bitumen obtained by a thermal cracking process. The "loss on heating" test results indicate that volatility at high temperatures is not greatly different for the two types of bitumen, but, from the reduction of penetration obtained in the test, the shale-oil bitumen appears to be less heat stable than the petroleum bitumens.

(2) *Viscosity–Temperature Characteristics*

A comparison of the viscosity-temperature characteristics of shale-oil and other bitumens (150/200 pen grade) was made over the temperature range 2° to 185° C. The results are given in Fig 1, where the logarithm of the absolute viscosity is plotted against the logarithm of the temperature in ° F. Viscosities in the temperature range 2°–60° C were measured in a coni-cylindrical viscometer [4] and from 60° to 185° C in a simple capillary tube viscometer.

The shale-oil bitumen has a significantly higher temperature coefficient of viscosity over the whole temperature range than the other bitumens. As a consequence, a 180/200 pen grade shale-oil bitumen can be sprayed satisfactorily at significantly lower temperatures than 180/200 pen grade petroleum bitumen, but has a higher viscosity at low road temperatures.

(3) *Brittleness and Visco-elastic Behaviour at Low Road Temperatures*

An important characteristic of a bituminous road binder is its response to rapid loading by traffic action at low road temperatures when its viscosity is high. A

good binder should absorb the energy of impact without breaking.

The brittleness of bituminous binders at low temperatures has been arbitrarily measured by means of an impact apparatus [5] in which a sample of binder is subjected to forces and rates of loading similar to those obtained on a road surface under a moving vehicle. In this test the temperature of the binder is reduced in

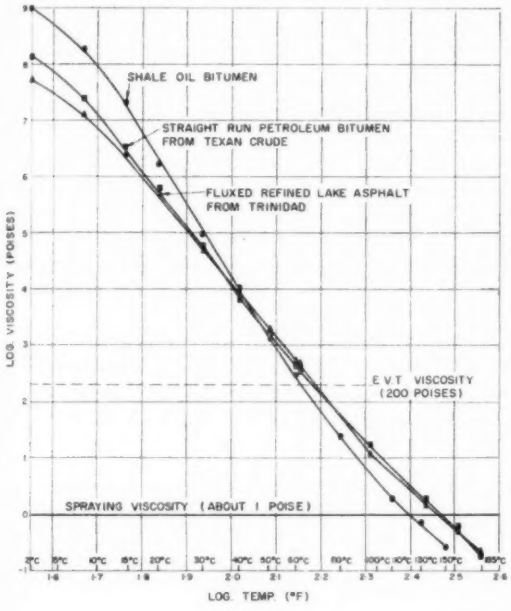
SHALE OIL BITUMEN
STRAIGHT RUN PETROLEUM BITUMEN FROM TEXAN CRUDE
FLUXED REFINED LAKE ASPHALT FROM TRINIDAD
E.V.T. VISCOSITY (200 POISES)
SPRAYING VISCOSITY (ABOUT 1 POISE)
LOG. VISCOSITY (POISES)
LOG. TEMP. (°F)

FIG 1

5° C steps until fracture occurs under impact. The so-called brittle temperature is partly dependent on the viscosity of the binder so that an arbitrary measure of brittleness can be obtained by the difference between the equi-viscous temperature (E.V.T.) and the brittle

TABLE VI

E.V.T. and Brittle Temperatures of 180/200 Pen Shale-oil and Other Bitumens

Bitumen	Grade	E.V.T. (° C)	Brittle temperature (B.T.) (° C)	E.V.T.–B.T.
Straight-run petroleum bitumen of Persian crude origin	40/50 pen	80	+5	75
Straight-run petroleum bitumen of Persian crude origin	180/200 pen	66	−10	76
Fluxed refined lake asphalt from Trinidad	180/200 pen	69	Lower than −15	Greater than 84
Shale-oil bitumen . . .	180/200 pen	58	−5	63

temperature. Results of brittleness tests on a shale-oil and other bitumens are given in Table VI.

According to this data, the shale-oil bitumen tends to be more brittle at low temperatures than the petroleum bitumen, which, in turn, is more brittle than the fluxed refined lake asphalt from Trinidad.

Kühn and Rigden [6] have investigated the visco-elastic behaviour of various types of bitumen under vibration loading and at temperatures in the range 0°–20° C. The behaviour at a frequency chosen to correspond with the short loading times encountered on a road surface under a moving vehicle was evaluated by means of a "merit" factor calculated from the measured real and imaginary parts of the elastic modulus. According to this "merit" factor the shale-oil bitumen would show greater brittleness at low road temperatures than straight-run petroleum bitumens of the same grade.

(4) *Stability to Heat Treatment*

An investigation has been done on the heat stability of various bitumens under conditions simulating the hot storage of a binder in a stirred binder heating tank.[7] In this study the criterion for overheating was taken to be an increase in viscosity greater than 40 per cent of the original. The maximum temperatures for storage for 15 and 24 hours in the binder heating tank without overheating were evaluated accordingly. The results of tests on different types of 180/200 pen grade bitumens are given in Table VII, together with

TABLE VII

Maximum Temperatures for Storage in a Field Binder Heating Tank

Bitumen (180/200 pen grade)	Maximum temperature of storage (° F)		Temperature (° F) at which viscosity is one poise
	For 15 hours	For 24 hours	
Shale-oil bitumen . .	285	275	251
Straight-run petroleum bitumen of Persian crude origin	600	585	330
Straight-run petroleum bitumen of Bahrain crude origin	600	580	313

temperatures at which the bitumens have a viscosity on one poise (approximately the spraying temperature).

These storage tests indicate that the shale-oil bitumen is significantly less heat stable than the petroleum bitumens. On the other hand, the shale-oil bitumen, having a higher temperature coefficient of viscosity, can be sprayed at a lower temperature than the petroleum bitumens, so that, in practice, there is no difficulty in handling the material if the recommended temperatures for storage and spraying are not exceeded.

(5) *Volatility at Road Temperatures*

Although bituminous binders of the "cutback" type are expected to lose lower boiling oils by evaporation when exposed on the road, any loss of the higher

boiling (plasticizing) oils of a binder will lead to undue hardening and is undesirable. "Straight-run" grades should show only a small loss by evaporation when exposed to temperatures near the maximum encountered on the road. Even with "cutback" type binders, however, evaporation of volatile oils is significantly retarded by the formation of a photo-oxidation skin on the exposed surface.[8]

Fig 2 compares the loss of oil from a 150/200 pen

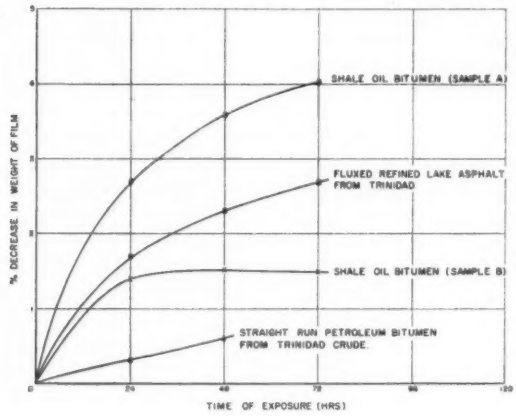
% DECREASE IN WEIGHT OF FILM
SHALE OIL BITUMEN (SAMPLE A)
FLUXED REFINED LAKE ASPHALT FROM TRINIDAD
SHALE OIL BITUMEN (SAMPLE B)
STRAIGHT RUN PETROLEUM BITUMEN FROM TRINIDAD CRUDE
TIME OF EXPOSURE (HRS)

FIG 2

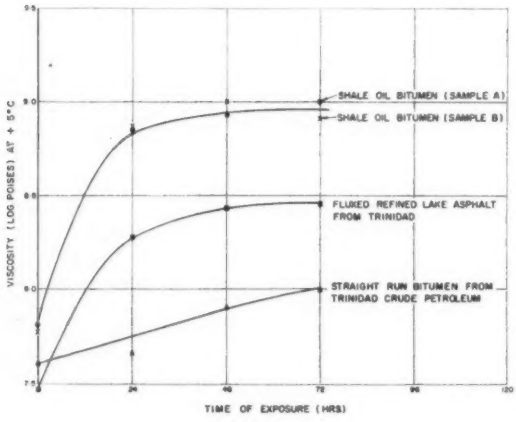
VISCOSITY (LOG POISES) AT + 5°C
SHALE OIL BITUMEN (SAMPLE A)
SHALE OIL BITUMEN (SAMPLE B)
FLUXED REFINED LAKE ASPHALT FROM TRINIDAD
STRAIGHT RUN BITUMEN FROM TRINIDAD CRUDE PETROLEUM
TIME OF EXPOSURE (HRS)

FIG 3

grade shale-oil bitumen and other 150/200 pen grade bitumens when both are exposed as films 0·6 mm thick at 70° C to a controlled stream of nitrogen. Fig 3 compares the increase in viscosity of the binders exposed under the same conditions. The viscosity was measured at +5° C in a "ball" viscometer developed to measure the viscosity of small samples of bituminous binders.[9] Under the conditions of test the shale-oil bitumen shows slightly greater hardening by evaporation than the other bitumens, but this hardening is not excessive, and the volatility characteristics of the material may be regarded as satisfactory.

(6) *Adhesion to Roadstone*

No detailed study has been made of the adhesion of shale-oil bitumen to roadstone, and the bitumen has given a satisfactory road performance in this respect. Like other bituminous binders, however, adhesion to most roadstones would be expected to be poor when liquid water is present at the bitumen–stone interface.

The rate of wetting of an "air-dry" and dusty roadstone in, for example, the surface dressing operation depends mainly on the viscosity of the binder at the surface of the binder film which comes into contact with the stone.

This will be determined primarily by the road temperature and, in the case of "cutback" type binders, may be influenced by partial evaporation of volatile oils. The short time of exposure of the film to light and oxygen between spraying and stone application may also produce some increase in the surface viscosity.

Other factors which may affect the rate of wetting of dusty roadstone by a bitumen are the formation of wax crystals on the surface of the bitumen and the presence of acidic material. Table VIII gives the

TABLE VIII

Wax Content and Acid Values of Shale-oil and Straight-run Petroleum Bitumens (150/200 *Pen Grade*).

	Shale-oil bitumen	Venezuelan bitumen	Persian bitumen	Saudi Arabian bitumen	Fluxed lake asphalt from Trinidad
Wax content % wt (modified Richardson's method)	1·5	0·4	4·3	3·2	0·2
Acid value ml $\frac{N}{10}$ (by potentiometric titration in benzene-methanol solvent)	less than 0·01	0·49	less than 0·01	0·02	1·03 (0·99 on benzene soluble part of bitumen)

results of wax content and acid value tests on shale-oil and straight-run petroleum bitumens (150/200 pen grade). The data given in Table VIII indicate that the wax content of the shale-oil bitumen is fairly low compared with some of the petroleum bitumens and that its acid value is negligible. The latter result would be expected because of the presence of lime in the bitumen introduced in the refining operation. (The shale-oil bitumen has an ash content of about 0·2 per cent by wt.)

The adhesion of shale-oil bitumen to dry roadstone would be expected to be reasonably good, particularly because of the low wax content and the presence of free lime and calcium salts (see p. 82).

(7) *Resistance to Oxidation at Road Temperatures*

Of the known causes of hardening of a bituminous binder when it is exposed in a road surfacing, loss of

plasticizing oils by evaporation and chemical attack by atmospheric oxygen are considered to be the most important. Two types of oxidation take place,[10] a rapid photo-oxidation on the exposed surface of the binder, which penetrates only a short distance into the surface, and a slower " thermal " reaction, which is partly controlled by the diffusion of oxygen into the binder. In most types of bituminous road surfacing it is the " thermal " reaction which is considered to be the most important cause of long-term hardening.

The susceptibility of binders to " thermal " oxygen attack can be assessed by an arbitrary test (the Pressure Oxidation Test [11]) involving the treatment of a film of binder 0·8 cm thick at 65° C with oxygen at a pressure of 300 psi and measuring the change in E.V.T. produced by the treatment. This test is known to have certain disadvantages, but serves as a rough guide to relative susceptibility to oxidation.

The results of pressure oxidation tests on a shale-oil bitumen and two other bitumens of the same grade are given in Table IX. On the basis of these results the shale-oil bitumen is more susceptible to oxidation than the other two bitumens, and it would be expected to be more prone to hardening by this factor on the road.

Results of the Survey of Properties

The survey of the physical and chemical properties of the shale-oil bitumen relevant to its use as a road binder has indicated that its relatively poor performance in pre-mix and surface treatment constructions compared with some petroleum bitumens is most probably due to inferior viscosity/temperature and brittleness characteristics and to a higher susceptibility to oxygen attack.

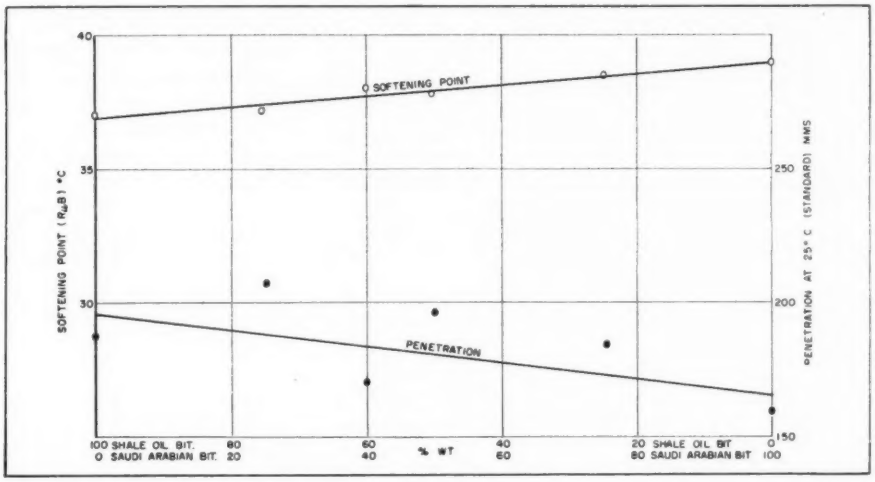

FIG 4

TABLE IX

Pressure Oxidation Test Results on Shale-oil and Other Bitumens

Bitumen	E.V.T.	Increase in E.V.T. on pressure oxidation	
		After 72 hours	After 210 hours
Shale-oil bitumen . . .	57·2	17·5	33·0
Straight-run petroleum bitumen from a Texan crude	66·0	7·4	11·0
Fluxed refined lake asphalt from Trinidad	66·1	12·3	26·0

Mapstone and Karius of the South African Torbanite Refining and Marketing Company Ltd [12] investigated methods for improving the viscosity/temperature characteristics of the bitumen and found that blowing with air at 400°–500° F in the presence of ferric chloride, or adding ferric chloride to the bitumen after blowing, produced an improved material. Further improvement could be obtained by fluxing the blown bitumen with acid fatty oils, although this type of flux did not always produce a homogeneous material. The road performance of these modified shale-oil bitumens has not been assessed.

The effect of blending on flow properties and susceptibility to oxygen attack has been investigated. A series of blends of a 150/200 pen grade shale-oil bitumen and a 150/200 pen grade straight-run bitumen from a Saudi Arabian crude petroleum were prepared and their softening point, penetration, and susceptibility to oxygen attack (as measured by the

pressure oxidation test) were determined. The results for the penetration and softening point tests are given in Fig 4 and the results of pressure oxidation tests are given in Fig 5.

For the properties tested, the effect of blending is roughly additive and the blends have properties intermediate between those of the two components, so that any improvement obtained by blending is roughly proportional to the amount of petroleum bitumen present.

As a start to an investigation of methods for reducing susceptibility to oxidation, a simple chemical examination was made of shale-oil bitumens recovered from old road surfacings and oxidized artificially in the laboratory.

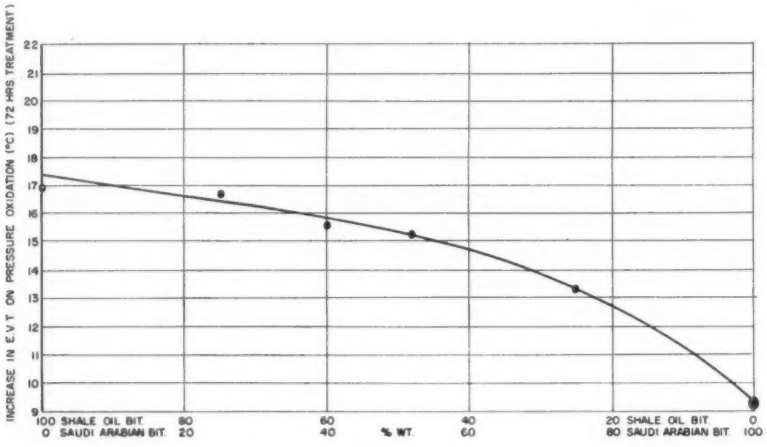

FIG 5

SIMPLE CHEMICAL EXAMINATION OF SHALE-OIL BITUMENS RECOVERED FROM OLD ROAD SURFACINGS AND OXIDIZED ARTIFICIALLY IN THE LABORATORY

Samples of six year-old pre-mix surfacings which had originally contained a 150/200 pen grade shale-oil bitumen were extracted with carbon disulphide and the soluble binder recovered from the solution by distillation. The E.V.T. of the binder was originally about 57° C, but the recovered binder from an untrafficked portion of the surfacing was found to have an E.V.T. of 94° C. For a trafficked portion the E.V.T. of the recovered binder was 79° C.

The recovered binder of 94 E.V.T., a fresh 150/200 pen grade shale-oil bitumen, and the same bitumen treated in the laboratory at 65° C for 210 hours under a pressure of oxygen of 300 psi were subjected to a simple chemical examination, the results of which are given in Table X. The bitumens were dissolved in benzene, extracted first with dilute alkali, and then with dilute sulphuric acid. The neutral fraction remaining was recovered from the solution and its unsaturation value determined by bromine absorption at +5° C.

The results obtained for the oxidized material show that oxygen at 65° C produces an increase of the benzene insoluble constituents and a reduction in the iodine value. A similar decrease in iodine value is obtained by exposure of the bitumen on the road, but since only the CS_2 soluble binder was recovered in this case, the true change in the benzene-soluble constituent may not be shown by the analysis.

TABLE X

Comparison of the Chemical Properties of a Shale-oil Bitumen Before and After Weathering on the Road, and After Oxidation in the Laboratory

Test	Fresh bitumen 150/200 pen grade	Weathered on the road for 6 years (originally 200 pen grade)	Oxidized for 210 hours at 65° C under an oxygen pressure of 300 psi
E.V.T. . . .	57	94	90
Insoluble in benzene (% wt)	4·5	2·5	10·7
Material extracted with 10% NaOH (% wt)	1·4	0·5	0·5
Material precipitated by alkali extraction (% wt)	1·6	Negligible	Negligible
Material extracted with 10% H_2SO_4 (% wt)	1·8	0·4	1·1
Material precipitated by acid extraction (% wt)	10·7	18·6	8·2
Iodine number of neutral fraction (by bromine absorption at +5° C)	81	69	68

The chemical examination, apart from indicating that the shale-oil bitumen undergoes considerable

oxidation when exposed on the road, suggests that the "unsaturated" compounds are consumed in the process and might be the reactive constituents towards oxygen.

On the assumption that the reactive "unsaturated constituents" might be polymerized or saturated by chemical treatment to produce a bitumen less susceptible to oxygen attack, various *ad hoc* treatments of the material were attempted.

AD HOC TREATMENTS TO REDUCE THE SUSCEPTIBILITY OF SHALE-OIL BITUMEN TO HARDENING BY OXIDATION

Attempts were made to polymerize the reactive constituents of the bitumen by treatment with aluminium chloride, benzoyl peroxide, stannic chloride, and acid sludge. Pressure oxidation tests before and after treatment indicated that treatment with these materials did not reduce the susceptibility of the bitumen to oxygen attack.

Treatment with 80 per cent sulphuric acid at 70°–80° C appeared to be more promising, and Table XI

TABLE XI

Pressure Oxidation Test Results on a 150/200 Pen Grade Shale-oil Bitumen Treated with 80 per cent Sulphuric Acid

Treatment of bitumen	Amount of heavy oil added to bitumen before treatment (to counteract the hardening produced by the treatment)	Increase in E.V.T. on pressure oxidation (72 hours)
None	None	17·5
+0·5% of 80% H_2SO_4	3·3	9·8
+1·0% of 80% H_2SO_4	6·5	7·2
+1·5% of 80% H_2SO_4	10·0	9·1

gives the pressure oxidation test results on a bitumen treated with various amounts of this reagent. Subsequent examination of the treated bitumen indicated that:

(*a*) all improvement obtained was destroyed by heat treatment at 150° C for 16 hours;

(*b*) all improvement obtained was destroyed by neutralization of the bitumen either with hydrated lime or caustic soda.

The behaviour of the sulphuric acid-treated bitumen to heating and alkali suggested that the change effected by the treatment was obtained by sulphation of "unsaturated" compounds rather than by polymerization, and attempts were therefore made to convert the "sulphates" into more stable derivatives. Generally the salts of sulphates are no more stable to heat treatment than the parent acids, but the alcohols obtained by hydrolysis are more resistant.

Working on this assumption, a fluxed 150/200 pen grade shale-oil bitumen was "sulphated" with 10 per cent sulphuric acid, hydrolysed, and extracted with water. An "improved" bitumen which was stable to heat treatment was obtained in one experiment when the treated bitumen was exhaustively extracted with water. In all other cases, however, where extraction was incomplete, unstable materials were obtained. The water extraction operation was found to be difficult, due to the formation of stable emulsions, and the method was abandoned as impracticable.

Finally, the effect of recognized petroleum antioxidants on the susceptibility of the bitumen to oxygen attack was investigated, but none of several compounds tested gave any significant improvement.

INVESTIGATION OF THE PRODUCTS OF THE REACTION OF OXYGEN WITH SHALE-OIL BITUMEN

Since *ad hoc* methods for reducing the susceptibility of the shale-oil bitumen to oxygen attack did not show much promise, it was decided to make a fairly detailed study of the products of the reaction between the bitumen and oxygen. Such a study might lead to the identification of the class of compounds mainly responsible for the high reactivity of the bitumen to oxygen and suggest methods for reducing reactivity.

A sample of 180/200 pen grade shale-oil bitumen was artificially oxidized by blowing a boiling solution of the bitumen in benzene (75° C) with air for 96 hours. The oxidized bitumen was recovered from solution and found to have increased in softening point (R and B) from 39·8° to 49·7° C.

Both the oxidized and unoxidized bitumens were then separated into fractions by a chromatographic method.

(1) *Chromatographic Method of Separation of Oxidized and Unoxidized Bitumen*

The bitumen (75 g) was dissolved in *n*-heptane, filtered, and introduced on to the top of a packed column of silica gel suspended in heptane. After elution with heptane (10 l) the heptane-insoluble part of the bitumen was introduced at the top of the column dissolved in benzene and the column was then eluted with benzene (8 l). After elution with benzene the column was eluted with pyridine (4 l).

The *n*-heptane and benzene eluates were recovered directly from solution by distilling off the solvent. The pyridine eluate was concentrated by distillation and precipitated in an excess of *n*-heptane to remove the remaining pyridine.

The amounts of each fraction isolated are given in Table XII. The separation process divided the

bitumens roughly into three equal parts, but oxidation did not greatly alter the distribution of these fractions. Some 3 per cent of the bitumen passed from the benzene eluate to the heptane eluate on oxidation.

TABLE XII

Amounts of Fractions Obtained From Chromatographic Separation of Oxidized and Unoxidized Shale-oil Bitumen

Bitumen	Unoxidized	Oxidized
Heptane eluate % wt (viscous oil)	33·7	37·3
Benzene eluate % wt (resin-like material)	35·1	32·3
Pyridine eluate % wt (brown powder)	26·8	27·6
Losses and residue on column % wt	4·4	2·8

(2) *Elementary Composition of the Bitumens and their Fractions*

Both the parent bitumens and the fractions derived from them were analysed for carbon, hydrogen, nitrogen, and sulphur (and ash) content to determine if oxidation produced any significant change in the distribution of these elements.

The atomic carbon–hydrogen ratio, the nitrogen and the sulphur contents of the oxidized and unoxidized bitumens, and the fractions separated from them by chromatography are given in Table XIII. The

TABLE XIII

Bitumen	Unoxidized	Oxidized
(a) *Atomic Carbon–Hydrogen Ratios of the Bitumens and their Fractions Before and After Oxidation*		
Total	0·89	0·90
Heptane eluate	0·78	0·76
Benzene eluate	0·92	0·92
Pyridine eluate	1·08	1·16
(b) *Nitrogen Contents of the Bitumens and their Fractions Before and After Oxidation (% wt of Ash-free Material)*		
Total	1·61	1·59
Heptane eluate	trace	trace
Benzene eluate	1·76	1·81
Pyridine eluate	3·10	2·89
(c) *Sulphur Contents of the Bitumens and their Fractions Before and After Oxidation (% wt of Ash-free Material)*		
Total	0·79	0·81
Heptane eluate	1·32	1·14
Benzene eluate	0·77	0·66
Pyridine eluate	0·90	0·82

atomic carbon–hydrogen ratio increased in the pyridine eluate and decreased slightly in the heptane eluate when the bitumen was oxidized, suggesting that the reaction is one of dehydrogenation with condensation (water evolved). There was no significant change in the distribution of the nitrogen and sulphur contents on oxidation, suggesting that compounds containing either of these elements are not particularly involved in the oxidation reaction. Chromatography tended to concentrate the sulphur compounds in the heptane eluate and the nitrogen compounds in the pyridine eluate.

(3) *Oxygen-containing Groups in the Bitumens and their Fractions*

Both the parent bitumens and their fractions were analysed for carboxyl, ester, carbonyl, and hydroxyl groups by the methods of Knotnerus.[13] The analysis procedure was complicated by the presence of lime in the bitumens and the pyridine eluate fractions, and this had first to be removed by extraction with aqueous hydrochloric acid. Despite thorough water washing, some hydrochloric acid remained in the extracted bitumen and fractions. This was determined separately from the weaker acids present, as two inflexion points were obtained in the potentiometric method used for measuring acid content.

TABLE XIV

Distribution of Oxygen Amongst Carboxyl, Ester, Carbonyl, and Hydroxyl Groups in the Oxidized and Unoxidized Bitumen and their Fractions

(a) *Unoxidized Bitumen*

Oxygen (% wt of total bitumen) present as the following groups:

	Carboxyl	Ester	Carbonyl	Hydroxyl	Total
Total bitumen *	0·22	0·66	0·11	0·57	1·56 (1·50% by diff in ultimate analysis)
Heptane eluate (34% by wt)	Nil	0·17	Nil	0·05	0·22
Benzene eluate (35% by wt)	Nil	0·27	0·13	0·32	0·72
Pyridine eluate * (27% by wt)	0·08	0·33	0·08	0·12	0·61
Total for eluates (96% by wt)	0·08	0·77	0·21	0·49	1·55

(b) *Oxidized Bitumen*

Oxygen (% wt of total bitumen) present as the following groups:

	Carboxyl	Ester	Carbonyl	Hydroxyl	Total
Total bitumen *	0·14	0·65	0·07	0·62	1·48 (2·01% by diff in ultimate analysis)
Heptane eluate (37% by wt)	Nil	0·35	0·06	0·04	0·45
Benzene eluate (32% by wt)	Nil	0·22	0·10	0·30	0·62
Pyridine eluate * (28% by wt)	0·18	0·31	Nil	0·15	0·64
Total for eluates (97% by wt)	0·18	0·88	0·16	0·49	1·71

* Extracted with aqueous HCl to remove any lime present.

The results of this analysis are given in Table XIV. The distribution of oxygen amongst the four types of group, both for the unoxidized and oxidized bitumens and their fractions, is given on a percentage weight basis calculated on the total bitumen.

Oxidation of the bitumen did not produce any significant increase in the amounts of the four oxygen-

containing groups estimated or any significant change in their distribution. A large part of the combined oxygen estimated in the bitumens was found to be present as hydroxyl and ester groups.

Examination of the distribution of the groups in the bitumen fractions showed that the chromatographic method of separation tended to concentrate the carboxylic acid constituents (as their calcium salts) in the pyridine eluate. The compounds containing hydroxyl groups tended, however, to concentrate in the benzene eluate and be present in only small concentrations in the heptane eluate.

A significant increase in ester content took place in the heptane eluate on oxidation, but this change was not confirmed by an increase in the ester content of the total bitumen.

Conclusions from the Chemical Investigation of the Products of the Oxidation of the Bitumens

Investigation of the products of the reaction of air (oxygen) with the shale-oil bitumen in benzene solution at 75° C did not give much positive information on the mechanism of the reaction or indicate the type of compound responsible for the relatively high oxygen reactivity.

It established that, under the experimental conditions, the reaction is mainly one of dehydrogenation and condensation without much formation of oxygen-containing products. There was some evidence that comparatively low molecular weight esters were formed in small quantity and that compounds containing nitrogen and sulphur were not playing an important part in the reaction.

GENERAL CONCLUSIONS

1. Carefully controlled road experiments have shown that South African shale-oil bitumen is less durable than certain petroleum bitumens and fluxed refined lake asphalt from Trinidad, but in certain constructions slightly more durable than some locally produced coke-oven tars. When the shale-oil bitumen is used as the binder for road wearing courses, either of pre-mix or surface dressing type, they have a shorter life than when petroleum bitumens are used.

2. The inferior durability of the shale-oil bitumen is due to its higher temperature susceptibility of viscosity and its tendency to become brittle at low road temperatures, and also to its high susceptibility to chemical attack by atmospheric oxygen when exposed in the wearing course of a road.

3. Chemical investigations of the properties of shale-oil bitumen, both weathered on the road and artificially oxidized in the laboratory, have given some information on the reaction of the bitumen with oxygen. The reaction appears to be mainly one of dehydrogenation and condensation of hydrocarbon components of the bitumen to give higher molecular weight products which increase its viscosity. There is some evidence that unsaturated hydrocarbons are among those which react with the oxygen and that some low molecular weight esters are among the products. Compounds containing nitrogen and sulphur do not appear to be important participants in the reaction.

4. Sulphation of the unsaturated hydrocarbons by low-temperature treatment with dilute sulphuric acid reduced the susceptibility of the bitumen to oxidation. The sulphated bitumen, however, decomposed when heated to normal handling temperatures and no practical means of overcoming this difficulty was found.

ACKNOWLEDGMENTS

This work was carried out as part of the programme of research of the Bituminous Binder Research Unit of the National Institute for Road Research and is published by permission of the South African Council for Scientific and Industrial Research.

The author wishes to thank members of the technical staff of the South African Torbanite and Refining Company Ltd for their co-operation and interest in the investigation. He also wishes to thank all his colleagues in the Bituminous Binder Research Unit, past and present, who were associated with the work.

References

1 Robertson, G. G. "Oil Shale and Cannel Coal," Vol. 2, p. 180. London: Institute of Petroleum, 1951.
2 "Full-Scale Road Experiments with Surface Treatments," Bulletin No. 2, National Institute for Road Research, South African Council for Scientific and Industrial Research, Pretoria, 1957.
3 "A Full-Scale Road Experiment with Pre-mixed Bituminous Carpets," Bulletin No. 3, National Institute for Road Research, South African Council for Scientific and Industrial Research, Pretoria, 1959.
4 Lee, A. R., Warren, T. B., and Waters, D. B. *J. Inst. Petrol*, 1940, **26**, 101–28.
5 Karius, H., and Dickinson, E. J. *J. Appl. Chem.*, 1959, **9**, 542–52.
6 Kühn, S. H., and Rigden, P. J. *Proc. Highway Res. Bd*, 1959, **38**, 431.
7 "Hot Storage of Bituminous Road Binders in the Field," Bulletin No. 4, National Institute for Road Research, South African Council for Scientific and Industrial Research (in preparation).
8 Mitchell, J. G., and Murdoch, D. G. *J. Soc. Chem. Ind.*, 1938, **57** (5), 137.
9 Kühn, S. H., and Rigden, P. J. *Proc. Ass. Asph. Pav. Technol.*, to be published.
10 Dickinson, E. J., Nicholas, J. H., and Boas-Traube, S. *J. Appl. Chem.*, 1958, **8**, 673.
11 Lee, A. R., and Dickinson, E. J. "The Durability of Road Tar." Road Research Technical Paper No. 31, HMSO, 1954.
12 Mapstone, G. E., and Karius, H. *J. Inst. Petrol.*, 1956, **42**, 361–9.
13 Knotnerus, J. *J. Inst. Petrol.*, 1956, **42**, 355–60.

REMOVAL OF IMPURITIES WHICH LOWER THE ELECTRICAL BREAKDOWN STRENGTH OF TRANSFORMER OIL BY DISTILLATION *

By M. DARVENIZA †

INTRODUCTION

It is generally agreed that the impurities which lower the electrical strength of insulating liquids are solid particles, water, and dissolved or entrained air. Repeated filtration and spraying at reduced pressure remove a large proportion of these impurities from transformer oil. For industrial purposes, this process is continued until the electric strength is raised above 40 kV as tested according to BS 148.[1] Investigations of the processes resulting in electrical breakdown require the best possible control of these impurities. This can be achieved only by their complete removal from the oil. The effect of each impurity on the breakdown strength of the oil may then be studied quantitatively by their separate introduction into the liquid in known concentrations.

Electric strength values, obtained by previous workers [2, 3] using filtration and spraying, are lower than might be expected by comparison with strengths obtained for pure hydrocarbon liquids [4] purified by normal distillation techniques. Purification of transformer oil by distillation does not seem to have been attempted, probably because this raises problems of oxidation and thermal decomposition due to its high boiling range. These problems have been overcome by flash distillation at reduced pressure.

Tests are described which determine the temperatures and pressures required for complete and efficient distillation of transformer oil. It is shown that the temperatures required are well below those which cause thermal decomposition, and that oxidation is avoided.

Dc electrical breakdown tests have been carried out to check the efficiency of purification and the results of these are compared with results previously reported. By varying the temperature of distillation, various fractions in the oil were separated and their electric strengths measured.

TEST EQUIPMENT AND APPARATUS

Oil Sample

Transformer oil conforming to BS 148 [1] was used in all tests. The oil was of Peruvian origin and consisted of 53·7 per cent C contained in paraffinic components, 37·8 per cent C in naphthenic, and 8·5 per cent C in aromatic components. The average mol wt was 310 and the density 0·88. The vapour pressure at 0° C was 10^{-4} mm Hg.

Gas Bubbling Chamber and Still

Meyers and Fenske [5] have shown that the relationship between boiling point and pressure for high-boiling hydrocarbons may be expressed:

$$\log P = A - \frac{B}{t + C}$$

where A, B, and C are constants, and P is in mm of Hg and is in ° C. From their data it was expected that the pressure would need to be reduced to less than 1 mm Hg to avoid thermal decomposition. To avoid oxidation, the oil was distilled in an atmosphere of nitrogen at the required pressure, and before distillation the oil was flushed with nitrogen to remove the oxygen, which is normally held in solution. The gas bubbling chamber consisted of a cylinder of approximately 2 l capacity, its base being a sintered glass filter of maximum porosity 10 μ. Gas was passed through the filter into the oil, thus giving a wide exposure of oil surface to the bubbling gas, and creating "froth" of oil. The top of the chamber was connected to the vacuum system, thus allowing preliminary degassing of the oil as well as removal of oxygen.

The still was of the vertical type and was designed for falling film distillation.[6] The distillation column is a 30 × 180 mm section of Pyrex tubing; on the inner surface ten turns of metal spiral forming the distilling surface are closely wound at a pitch of about 15°. Condensation of the vapour is on a water-conducting tube of 3 mm bore, concentric with the distilling surface and extending through both ends of the still. The temperature of the distilling surface is controlled by means of an external heating jacket. Temperatures up to 300° C were measured by a thermocouple inserted between the still and the heating jacket. A schematic diagram of the apparatus is shown in Fig 1.

* MS received 25 March 1959.
† University of Queensland, St. Lucia, Brisbane, formerly at Queen Mary College, University of London.

Vacuum System

The still was connected with wide-bore tubing to a diffusion pump vacuum system, including a liquid air trap. The pressure in the still was controlled by adjusting a leak rate of dry nitrogen with a fine

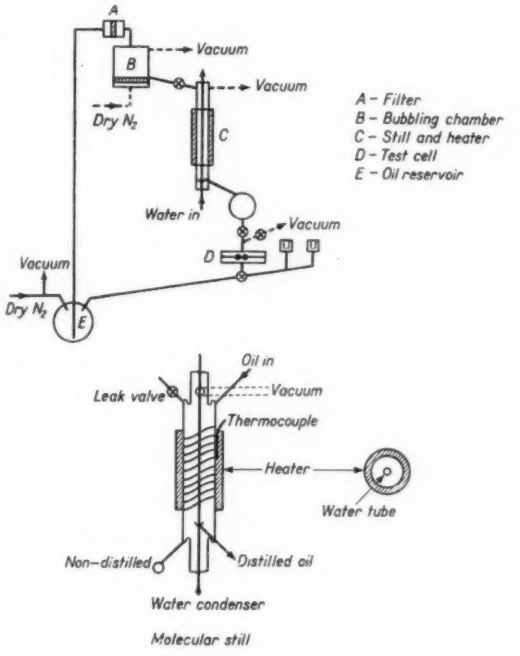

FIG 1

LAYOUT OF STILL AND LIQUID APPARATUS

control needle valve. The pressure in the system was measured with a Pirani gauge calibrated in nitrogen. A vacuum of less than 10^{-4} mm Hg was achieved in all parts of the system.

Test Cell and Electrical Equipment

Breakdown measurements were made between 1 cm diameter nickel spheres (mounted horizontally) in a test cell of volume less than 50 ml. The electrodes were buffed with soft mops and a suitable grease until microscopic observation showed no pits or scratches on the sparking areas. The gap was adjusted with a micrometer in the range 75–125 μ. In this range it was shown that the electric strength was not dependent on gap length.

An 18-kV dc supply was used, and the voltage applied to the test cell was measured with a calibrated resistance chain and micro-ammeter and is considered accurate to within ±1·5 per cent. The rate of rise of voltage applied to the test cell was sufficiently slow to make the breakdown measurement independent of time. It was found that the rates less than 450 V/sec had no significant effect on the breakdown value.

Breakdown products and damage to electrodes were kept as low as possible by diversion, using a hydrogen thyratron which shorted the test cell 0·5 microsec after breakdown. This diversion greatly reduced scatter in breakdown measurements.

EXPERIMENTS

Operation of Still

The oil was filtered into the gas bubbling chamber through a sintered glass filter of maximum pore size 1 μ. The oxygen in solution was removed by flushing the oil with oxygen-free nitrogen for at least 48 hours. Subsequent experiments, which measured the effect of minute quantities of oxygen on the electric strength of the oil,[7] indicated that this flushing was sufficient to remove all traces of free oxygen. Before distillation, the oil was allowed to settle into rough equilibrium with the intended distillation pressure whilst in the bubbling chamber. This ensured that no violent degassing (in the form of bursting bubbles) took place as the film of oil was allowed to run on to the distilling surface. The flow of liquid into the still was carefully controlled so that it followed the path of the spiral. Since the process of flash distillation is essentially evaporation from the surface of the liquid, it was essential to achieve a smooth film, spread evenly over the entire evaporating surface.

The rate of distillation is controlled by the satisfactory formation of an even film on the metal spiral, and it was found that a rate of about 100 ml/hr could not be exceeded.

Temperatures and Pressures Required for Distillation

The temperature at which the lighter fractions of oil began to boil at atmospheric pressure was determined and was 310° C.

Distillation of measured quantities of the oil was carried out at various temperatures with a pressure of 4×10^{-2} mm Hg maintained in the still. At each test the proportion of oil distilled was determined by mass measurements and is shown plotted against still temperature in Fig 2. Distillation of the lighter fraction began at 50° C. At 85° C roughly half the liquid had distilled. At 140° C less than 1 per cent remained undistilled. The mass of this portion could not be measured accurately from 140° to 200° C because the quantity was very small and the liquid left on the glass surfaces by wetting made accuracy impossible. However, it was noted that the portion of the oil not distilled at 140° C consisted mostly of the coloured components of the oil. Visual observa-

tion showed that these components were distilled at 210° C. The temperature required varied somewhat with the rate of distillation, probably because of improved separation at lower rates.

A Pulfrich refractometer capable of measuring to the fifth decimal place was used to measure the refractive index of the oil during these tests. At temperatures below 200° C the refractive index was found to be lowered, indicating the separation of the higher boiling point components. With a distillation temperature of 210° C no change in refractive index was recorded, the value corrected for temperature to 20° C being 1·47791 using the sodium D line.

The temperatures required for distillation were determined for pressures of 4×10^{-2}, 10^{-1}, and 1 mm of Hg. The values are plotted in Fig 3 in the manner $-\log P$ *v.* $1/t + 230$. Results from data given by Meyers and Fenske [5] were used to give the form of

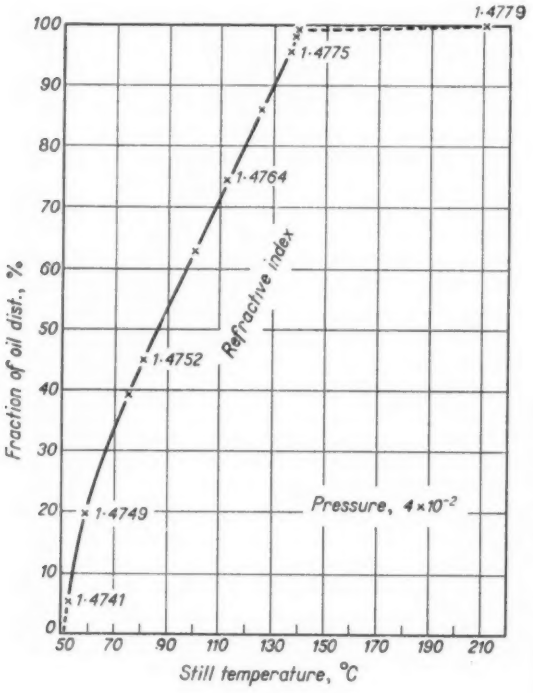

FIG 2

PROPORTION OF OIL DISTILLED AS A FUNCTION OF TEMPERATURE AT A PRESSURE 5×10^{-3} mm Hg

the curves for transformer oil, since only three points on each curve were determined experimentally. This is justified, as they have shown that all high boiling point hydrocarbons behave in a similar fashion in this range.

Thermal Decomposition and Oxidation

Two stills were available: one using a platinum spiral for the distilling surface and the other a nickel spiral. Distillation of many litres of oil with the

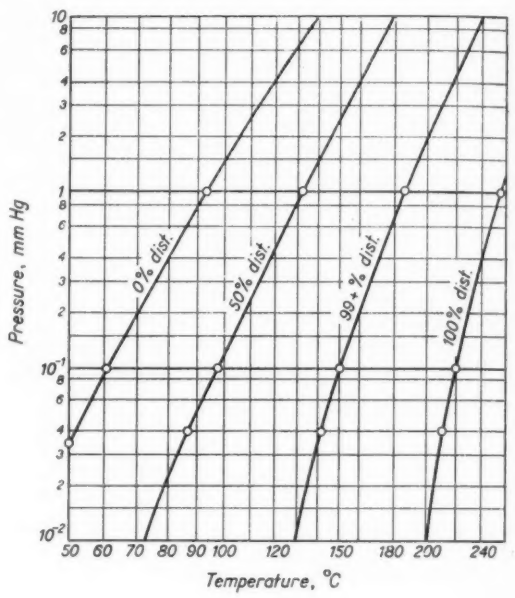

FIG 3

BOILING POINT OF VARIOUS FRACTIONS AS A FUNCTION OF PRESSURE IN THE STILL

platinum still showed no evidence of degradation products left on the distilling surface. However, with the nickel still, distillation of a similar quantity of oil revealed a small quantity of degraded products left on the distilling surface. These were washed from the surface, and it is estimated that about 0·5 ml was collected from the distillation of 2 l of oil.

Using the platinum still, a sample of oil was distilled repeatedly at a temperature of 270° C. After ten distillations no variation in the refractive index from 1·47791 was recorded. This indicated that no significant change in the molecular structure of the components in the oil would occur at the lower temperatures used in the distillation of samples for breakdown tests. It must be noted that the refractive index of this oil varied in the fourth decimal place with samples taken from different drums.

As was expected from the care taken to exclude oxygen from the system, no obvious oxidation products were observed. As a rough check, distillation was carried out in an air atmosphere, and white clouds of oxidation products were formed in the still

with air pressures in excess of 10 mm of Hg. Conduction current measurements in oil distilled in an inert atmosphere confirmed that negligible oxidation occurred during distillation.

Electrical Breakdown Measurements

Oil was distilled at a temperature of 220° C and then directed into the test cell, which had been evacuated for a period of at least 8 hr. Electrodes were buffed with soft mops, using suitable polishing compounds, and were degreased in hexane before placing in the test cell. To remove particles, the test cell was flushed with oil at least twice before breakdown measurements were made.

No significant variation in the electrical breakdown strength of the oil was recorded if the pressure of nitrogen in the still was varied from 5×10^{-3} to 1 mm Hg. Tests were carried out at eight intermediate pressures, and the average breakdown stress achieved was 1130 kV/cm, with a scatter of 4·8 per cent. These values are the mean of at least 25 breakdown shots taken after the conditioning process [2, 3] was complete in each test. The breakdown strength of the oil before entry into the system was measured to be 380 kV/cm, with a scatter of 8·2 per cent.

The breakdown strength of different fractions of the oil was measured by altering the distillation temperature. Table I gives the strength values over a range of temperatures with a pressure of 10^{-1} mm Hg of nitrogen in the still.

TABLE I

Electric Strength of Various Fractions of Transformer Oil

Still temp, ° C .	240	210	158	145	120	80
% oil distilled .	100	>99	>99	93	72	35
Electric strength, kV/cm . .	1130	1130	1210	1320	1320	1320

DISCUSSION OF RESULTS

The high dc strength of 1130 kV/cm obtained for distilled oil is an indication that the technique used achieved efficient purification of the oil. By comparison, a breakdown strength of 140 kV/cm is required by BS 148 [1] for transformer oil, and values of 730 kV/cm were reported by El-Dine and Tropper.[2] Khambanonda [3] obtained strengths of 1120 kV/cm with a glass system which completely sealed the oil from the atmosphere at all times after prolonged degassing and filtration at a vacuum of 3×10^{-2} mm Hg.

These comparisons confirm that one cycle of distillation removes deleterious impurities; it is of importance to estimate the concentration of impurities left in the oil. It is difficult to estimate the removal of solid particles because of the small distance (13 mm) travelled by the oil in the vapour phase. Since the components of the oil boil over a wide range, there will be a tendency for the lower boiling point molecules to leave the distilling surface with sufficient kinetic energy to carry small particles across the gap.

Removal of gas and moisture from the oil during distillation must be very effective because of the intimate exposure of the oil molecules in their vapour state to the vacuum held in the still. Transformer oil in equilibrium with air at atmospheric pressure contains 10 per cent by volume of air in solution, *i.e.* 135 ppm by weight. Kaufmann *et al.*[8] have shown that the air content of oil obeys Henry's Law, *i.e.* a linear relationship exists between equilibrium pressure and the gas content of the oil. The gas content of the oil distilled at a pressure of 10^{-2} mm Hg would be reduced by $10^{-2}/760$. Thus the oil condensing in equilibrium with this pressure would have a theoretical gas content of less than 1 in 10^8.

Similarly, Kaufmann [8] has shown that water dissolved in transformer oil follows the classical laws for dilute solutions. The maximum water solubility, *i.e.* the water content of oil in equilibrium with the saturated vapour pressure of water at 20° C (17·5 mm Hg) is approximately 40 ppm. If oil of this maximum water content was distilled at a rate of 100 ml/hr with a total pressure of 10^{-2} mm Hg maintained in the still the partial pressure of water vapour is estimated at 10^{-3} mm Hg with a liquid air trap in the system. Thus the moisture content of the oil condensing is theoretically less than 1 in 10^8.

It has been shown (Table I) that the breakdown strength of the liquid was raised if the high boiling point components of the oil were removed by fractional distillation. Subsequent investigations indicated that the rise in electric strength was associated with the removal of fluorescent materials normally present in transformer oil. It was observed that light was emitted from the oil gap by the action of high electric stress.[9] Fractional distillation at a temperature of 145° C in a nitrogen pressure of 10^{-1} mm Hg partially removed the fluorescent materials, and this resulted in a decrease in light output and an increase in electric strength. Because of the inherent complexity of the natural mixture collectively called transformer oil, no detail about the exact nature of the material removed by distillation can be given.

CONCLUSIONS

A technique of flash distillation at reduced pressure has been applied to the purification of the transformer oil producing 50 to 100 ml of clean oil per hour. It

has been shown that distillation of the oil is possible with negligible decomposition, and that high electric strength may be attained with one cycle of distillation. Where relatively small quantities of dielectric are required, distillation purification of transformer oil offers a means of providing a high-strength insulating fluid.

ACKNOWLEDGMENTS

The author is indebted to Dr. H. Tropper for his helpful encouragement and to Professor Humphrey Davies for facilities provided at Queen Mary College, University of London. The award of a Travelling Research Fellowship by the University of Queensland is gratefully acknowledged.

References

[1] BS 148 : 1959.
[2] El-Dine, Z., and Tropper, H. *Proc. Instn elect. Engrs Monograph* S 135, June 1955.
[3] Khambanonda, A. Ph.D. thesis, London University, 1958.
[4] Lewis, T. J. *Proc. Instn elect. Engrs*, 1953, **100** (11A), 141.
[5] Meyers, H. S., and Fenske, M. R. *Industr. Engng Chem.*, 1955, **47**, 1658.
[6] Breger, I. A. *Analyt. Chem.*, 1948, **20**, 980.
[7] Darveniza, M. Ph.D. thesis, London University, 1959.
[8] Kaufmann, R. B., *et al. Trans. Amer. Inst. elect. Engrs*, 1955, **74**, 312.
[9] Darveniza, M. *Nature, Lond.*, 1959, **183**, 743.

TECHNICAL NOTE

ESTIMATION OF RELATIVE MAXIMUM DEPTHS OF BURIAL*

By G. D. HOBSON† (Fellow)

In trying to solve geological problems in some types of area, information on the relative amounts of cover which have been removed at different points can be of value. Thus, from this information, indications may be obtained of the amount of regional tilting, or of possible differences in maximum temperature and pressure due to differences in maximum depth of burial, and these may account for differences of post-depositional origin in the characteristics of the rocks.

Shales and clays are subject to compaction on burial; their porosity diminishes as their depth of burial increases, and correspondingly the bulk density increases. This change in density, which must be linked with changes in elasticity, is associated with a change in the velocity with which seismic impulses are transmitted through these rocks. The velocities increase as the depth of burial increases, and time/depth curves are of the form shown in Fig 1 (*a*).

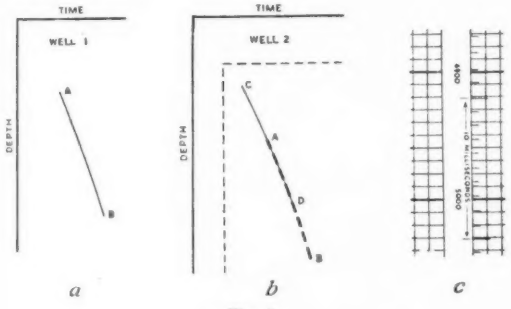

FIG 1

(*a*) TIME/DEPTH CURVE SHOWING INCREASE IN VELOCITY WITH DEPTH
(*b*) TIME/DEPTH CURVE OF WELL 1 (A, B) SUPERIMPOSED ON THAT FOR WELL 2 (C, D) WITH THE SLOPES MATCHING
(*c*) PART OF DEPTH MARKINGS ON A SONIC LOG SHOWING INTEGRATED TIME MARKS ON THE RIGHT-HAND SIDE

It is evident that depth/load relationships depend on the nature of the rocks forming the load and on their degree of compaction. Furthermore, the temperature gradient also depends on the nature of the rocks. These points must be borne in mind when making deductions from estimates of former differences in load.

When strong folding has taken place it is possible that the stresses will have disturbed the simple depth/porosity relationships for a shale envisaged in an earlier paragraph. There may be a comparable disturbance near a substantial fault.

If for two localities a shale is of a given type and it is, and also has been, equally loaded at the two localities by burial, the time/depth curves can be expected to be identical. However, in the absence of complete recovery on removal of load, if there were differences in maximum load, but these differences involved differences in burial appreciably less than the thickness of the shale, the time/depth curve for the upper part of the shale at the locality of deeper burial should be identical in form with the time/depth curve for the lower part of the shale at the locality of less maximum burial. Thus, in principle, matching of slopes of the curves (Fig 1 (*b*)) could give indications of similarity in maximum load on the given shale sectors, and hence more approximately of similarity in maximum depth of burial. Consideration of any vertical shift of the time/depth curves needed to give the match would afford evidence of changes between the maximum and current relative depths of burial of the shale for the places in question.

For many years velocity shooting has been carried out in wells, and this has provided time/depth curves. However, the nature of velocity shooting is such that the definition of the curve for a formation is subject to some uncertainty, and it is normally dependent on a small number of widely spaced points. As a result the deductions which could be made from matching would be subject to considerable uncertainty, unless the formation (shale) is exceptionally thick.

Within the past few years sonic logging of boreholes has been introduced in oilfield areas, and logs can now be obtained on which the integrated time is marked by a series of pips [2] (Fig 1(*c*)). Such logs would appear to make the problem of matching straightforward, for the logs of the relevant part of the rock sequence in a pair of wells would merely have to be slid over each other until a succession of pips agreed in spacing in detail. Naturally it would be necessary to be assured of lithological similarity, and normally identicality in age, for the given formation at the wells considered. Evidence of this could be

* MS received 7 January 1960.

† Department of Geology, Imperial College, London.

obtained from electric and radioactivity logs, as well as from cores.

When no matching was possible, deductions might still be drawn about the minimum difference in original load.

If there is recovery (and an equivalent effect on the seismic velocity) of the shale on removal of overburden this could affect the accuracy of the approach suggested. This effect may exist in some degree. A. W. Skempton has published a diagram [1] which suggests a small recovery in the case of London Clay on the removal overburden.

Seismic wave speeds are stated to be proportional to the square root of the elasticity of the rock, and inversely proportional to the square root of the density. Skempton's diagram gives an indication of a slight change in density, but affords no evidence of the extent of a change, if any, in the elasticity of the clay. Well velocity shooting data have indicated that the seismic velocities for a given shale do not necessarily agree at what are currently the same depths, so it would appear that the recovery is by no means complete. However, to the extent that it occurs it will lead to added uncertainty in the figures obtained by the procedure proposed. The error due to this factor may well be small, because it will be the differences in the recovery factors which will be involved.

References

[1] Skempton, A. W. *Quart. J. Geol. Soc. Lond*, 1944, **100**, 119–35.

[2] Tixier, M. P., Alger, R. P., and Doh, C. A. *J. Petrol. Tech.*, May 1959, **11** (5), AIMME Tech. Paper No. 8063, 106–14.